Author's personal copy

1.02 Fundamental Point Defect Properties in Ceramics☆

Patrick A Burr, University of New South Wales, Sydney, Australia
Michael JD Rushton, Bangor University, Bangor, United Kingdom
Alexander Chroneos, Coventry University, Coventry, United Kingdom
Robin W Grimes, Imperial College London, London, United Kingdom

© 2020 Elsevier Ltd. All rights reserved.

1.02.1	**Introduction**	50
1.02.2	**Intrinsic Point Defects in Ionic Materials**	51
1.02.2.1	Point Defects Compared to Defects of Greater Spatial Extent	51
1.02.2.2	Kröger Vink Notation	51
1.02.2.3	Charge of Point Defects	51
1.02.2.4	Intrinsic Disorder Reactions	52
1.02.2.5	Concentration of Intrinsic Defects	54
1.02.3	**Defect Reactions**	55
1.02.3.1	Intrinsic Defects	55
1.02.3.2	Effect of Doping on Defect Concentrations	56
1.02.3.3	Decrease of Intrinsic Defect Concentration Through Doping	56
1.02.3.4	Defect Associations	56
1.02.3.5	Non-Stoichiometry	58
1.02.3.6	Peroxide Accommodated Hyper-Stoichiometry	59
1.02.3.7	Lattice Response to a Defect	59
1.02.3.8	Defect Cluster Structures	60
1.02.4	**Electronic Defects**	62
1.02.4.1	Formation	62
1.02.4.2	Concentration of Intrinsic Electrons and Holes	63
1.02.4.3	Band Gaps	64
1.02.4.4	Excited States	64
1.02.5	**The Brouwer Diagram**	66
1.02.5.1	Defects With Formal Charge States	66
1.02.5.2	Oxidation States of Defects	67
1.02.6	**Transport Through Ceramic Materials**	69
1.02.6.1	Diffusion Mechanisms	69
1.02.6.2	Diffusion Coefficient	71
1.02.7	**Summary**	72
1.02.8	**Recommended Reading**	72
References		73

1.02.1 Introduction

The mechanical and electronic properties of crystalline ceramics are controlled by the point defects they contain. As a consequence, it is necessary to understand the structures, energies and concentration of defects and their interactions.[1,2] In terms of their crystallography it is often convenient to characterize ceramic materials by their anion and cation sublattices. Such models lead to some obvious expectations. It might, for example, be energetically unfavorable for an anion to occupy a site in the cation sublattice and vice versa. This is because it would lead to anions having nearest neighbor anions with a substantial electrostatic energy penalty. Further, there should exist an equilibrium between the concentration of intrinsic defects (such as lattice vacancies) extrinsic defects (i.e., dopants) and electronic defects in order to maintain charge neutrality.[1,2] Such constraints on the types and concentrations of point defects are the focus of this article.

In the first section we will consider intrinsic point defects in ionic materials. This will be followed by a discussion of the defect reactions describing the effect of doping, defect cluster formation and nonstoichiometry. Thereafter we will consider the importance of electronic defects and their influence on ceramic properties. The first three sections will be combined by introducing a generalised

☆*Change History*: December 2019. Patrick A. Burr, Michael J.D. Rushton, Alexander Chroneos and Robin W. Grimes has updated several sections, with the addition of new figures, to reflect recent research progress. The order of some sections was restructures for the benefit of clarity, and the sections of defect transport and oxidation states were significantly augmented.
This is an update of Chroneos, A., Rushton, M.J.D., Grimes, R.W., 2012. Chapter 1.02 – Fundamental Point Defect Properties in Ceramics. In: Konings, R.J.M. (Ed.), Comprehensive Nuclear Materials, Elsevier, pp. 47–64.

 doi:10.1016/B978-0-12-803581-8.11787-4

Author's personal copy

method to predict concentrations of intrinsic, extrinsic, clustered and electronic defects. In the final part, we are concerned with solid state diffusion in ceramic materials. Examples will be used throughout to illustrate the extent and range of point defects and associated processes occurring in ceramics. Subsequent chapters will deal with defects of greater spatial extent, such as dislocations and grain boundaries, however here we will begin by comparing them with point defects.

1.02.2 Intrinsic Point Defects in Ionic Materials

1.02.2.1 Point Defects Compared to Defects of Greater Spatial Extent

In crystallography we learn that the atoms and ions of inorganic materials are, with the exception of glasses, arranged in well defined planes and rows.[3] This is, however, an idealized representation. In reality, crystals incorporate many types of imperfections or defects. These can be categorized into three types depending on their dimensional extent in the crystal:

(1) Point defects, which include missing atoms (i.e., vacancies), incorrectly positioned atoms (e.g., interstitials) and chemically inappropriate atoms (dopants or substitutions). Point defects may exist as single species or as small clusters consisting of a number of species.
(2) Line defects or dislocations extend through the crystal in a line or chain. The dislocation line has a central core of atoms which are located well away from usual crystallographic sites (in ceramics this extends, in cylindrical terms, a nanometer or so). Dislocations can be of edge, screw or mixed type.[4]
(3) Planar defects extend in two dimensions and are atomically, or nearly atomically, thin in only one direction. Many different types exist the most common of which is the grain boundary. Other common types include stacking faults, inversion domains and twins.[1,2]

What has been described above are the chemical or simple structural models for the extent of defects. It is critical to bear in mind that all defect types, in all materials, may exert an influence via an electrostatic and/or elastic strain field that extends well beyond the chemical extent of the defect (i.e., beyond those atoms replaced or removed). This is because the lattice atoms surrounding the defect have had their bonds disrupted. Consequently these atoms will accommodate the existence of the defect by moving slightly from their perfect lattice positions. These movements in the positions of the neighboring atoms are referred to as lattice relaxation.

As a result of the elastic strain and electrostatic potential (if the defect is not charge neutral), defects can affect the mechanical properties of the lattice. In addition, defects have a chemical effect, changing the oxidation/reduction properties. Defects also provide mechanisms for or impede the movement of ions through the lattice. Finally, defects will alter the way that electrons interact with the lattice, since defects can alter the potential energy profile of the lattice (whether or not the defect is charged). This may lead to trapping of electrons. Also, since dopant ions will have a different electronic configuration than the host atom, defects may donate an electron to a conduction band resulting in n-type conduction or a defect may introduce a hole into the electronic structure resulting in p-type conductivity.

1.02.2.2 Kröger Vink Notation

It is usual for defects in ceramic materials to be described using a short-hand notation after Kröger and Vink.[5] In this, the defect is described by its chemical formula. Thus, a sodium ion would be described as Na, whatever its position in whatever lattice. A vacancy is designated as "V" or sometimes "v". A subscript describes the position within the lattice that the defect occupies. For example, a vacant Mg site is designated V_{Mg} and a Na substituted at an Mg site is designated $\mathrm{Na_{Mg}}$. Interstitial ions are represented as "i" so that an interstitial fluorine ion in any lattice would be F_i.

The charge on an ion is described with respect to the site that the ion occupies. Thus a Na ion (which has formal charge $+$) sitting on an Mg site in MgO (which expects to be occupied by a $2+$ ion) has one too few $+$ charges; it has a relative charge of 1 – which is designated as a slash /, meaning that it is written as: $\mathrm{Na}^{/}_{\mathrm{Mg}}$. An Al^{3+} ion at an Mg site in MgO has too high a charge. Positive excess charge relative to a site is designated with a dot, thus $\mathrm{Al}^{\bullet}_{\mathrm{Mg}}$. Similarly, a vacant Mg site in MgO is designated as $V^{//}_{\mathrm{Mg}}$ and an interstitial Mg ion in MgO as $\mathrm{Mg}^{\bullet\bullet}_i$. Finally, a neutral charge is indicated by a cross "$\times$", so that a Mg ion at a Mg site in MgO is $\mathrm{Mg}^{\times}_{\mathrm{Mg}}$.

Ions such as Fe may assume more than one oxidation state. Therefore, in MgO we might find both Fe^{2+} and Fe^{3+} ions on Mg sites; that is, $\mathrm{Fe}^{\times}_{\mathrm{Mg}}$ and $\mathrm{Fe}^{\bullet}_{\mathrm{Mg}}$. It is also possible to encounter bound defect pairs or clusters. These are indicated using curly brackets and an indication of the overall cluster charge, for example, an Fe^{3+} ion bound to a Na^{+} ion, both substituted at magnesium sites would be: $\left\{\mathrm{Fe}^{\bullet}_{\mathrm{Mg}} : \mathrm{Na}^{/}_{\mathrm{Mg}}\right\}^{\times}$. Square brackets instead indicate concentrations of the defect, thus the concentration of Fe^{3+} ions substituted at magnesium sites in MgO would be $[\mathrm{Fe}^{\bullet}_{\mathrm{Mg}}]$. The nomenclature is summarized in Fig. 1.

Finally, when we consider free electrons or holes, these are commonly represented as $e^{/}$ and $h^{\bullet}$ respectively, and their concentration is typically represented by n and p. When the electron or hole is localized on a specific atom, it is represented by a charged atomic defect, for instance a Fe^{3+} atom in FeO (in which Fe atoms are expected to have a $2+$ charge) is $\mathrm{Fe}^{\bullet}_{\mathrm{Fe}}$. These are also known as small polarons.

1.02.2.3 Charge of Point Defects

Most ceramics are ionic crystals, and as such the constituent atoms are typically fully iodized. For instance, MgO is comprised of Mg^{2+} and O^{2-} ions. These are known as the *formal* charge states. When oxygen vacancies are produced in MgO, they will have an

Author's personal copy

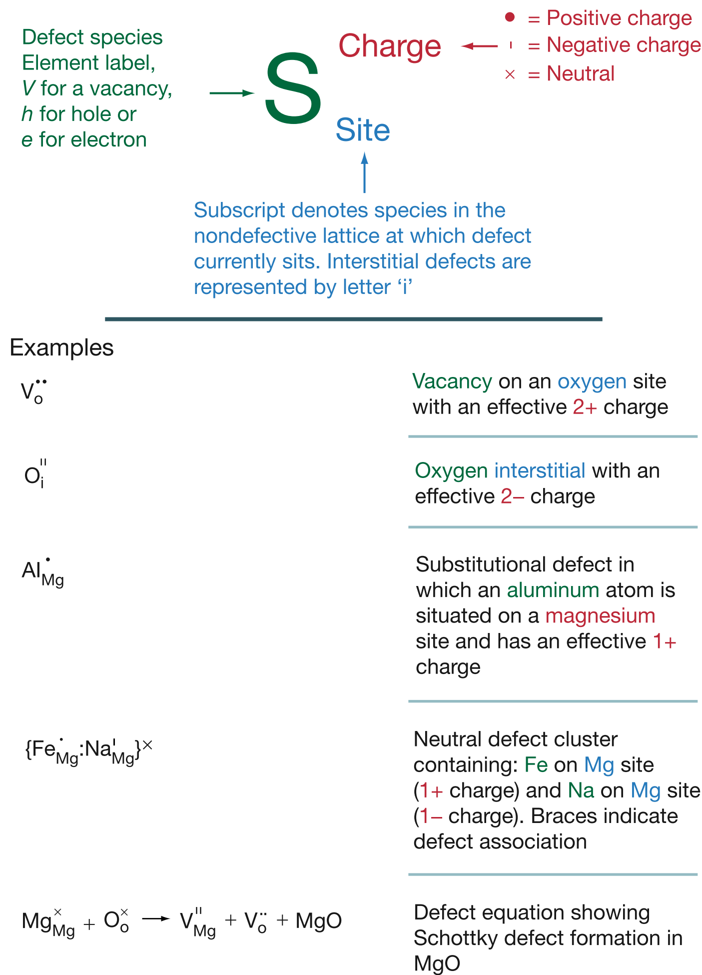

Fig. 1 Overview of Kröger-Vink notation.

effective charge (i.e., compared to the background crystal field) of 2+, denoted $V_O^{\bullet\bullet}$, as discussed above. However, defects do not always retain their formal charge, in other words they are not always ionized to their highest oxidation state. This is particularly relevant for partly covalent ceramics (e.g., BeO), for semiconductors, and for ceramics exposed to electrochemical potentials (such as oxidation and anodization). In these cases, the charge state of the defects will depend on the chemical potential of the electrons. This will be discussed in greater detail in Section 1.02.5.2, after the introduction of defect reaction with formal charges (in Section 1.02.3) and a description of electronic defects (Section 1.02.4).

1.02.2.4 Intrinsic Disorder Reactions

A number of different point defects can form in all ceramics but their concentration and distributions are interrelated. In the event of the production of a vacancy, for example, by the displacement of a lattice atom, this released atom can be either contained within the crystal lattice as an interstitial species (forming a Frenkel pair) or migrate to the surface to form part of a new crystal layer (resulting in a Schottky reaction). **Fig. 2** represents a Frenkel pair: both cations and anions can undergo this type of disorder reaction, resulting in cation Frenkel and anion Frenkel pairs respectively. In ceramic materials both the vacancy and interstitial defects are usually charged but the overall reaction is charge neutral. The energy necessary for this reaction to proceed is the energy to create one vacancy by removing an ion from the crystal to infinity plus the energy to create one interstitial ion by taking an ion from infinity and placing it into the crystal. The implication of removing and taking ions from infinity implies that the two species are infinitely separated in the crystal (unlike the two species shown in **Fig. 2**). As separated species these are defects at infinite dilution, a well defined thermodynamic limit. Since the two defects are charged, they will interact if not infinitely separated, a point we will return to later.

As with the Frenkel reaction, the Schottky disorder reaction must be charge neutral. Here only vacancies are created but in a stoichiometric ratio. Thus, for a material of stoichiometry AB, one A vacancy and one B vacancy are created, as shown in **Fig. 3**. The displaced ions are removed to create a new piece of lattice. It is important to realize that we are dealing with an equilibrium

Author's personal copy

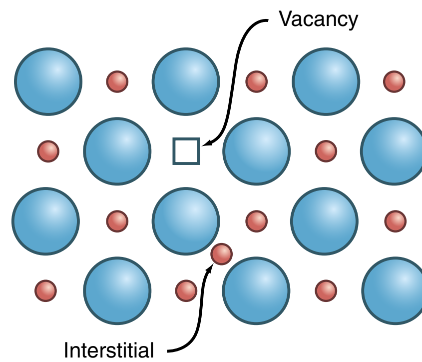

Fig. 2 Schematic representation of a Frenkel pair in a binary crystal lattice.

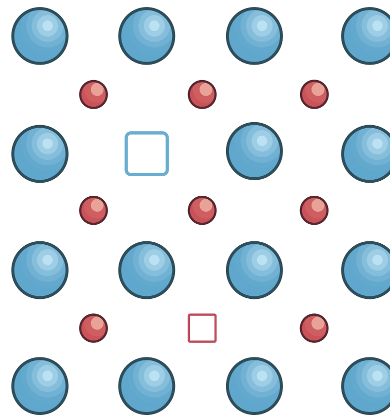

Fig. 3 Schematic representation of a Schottky pair in a binary crystal lattice.

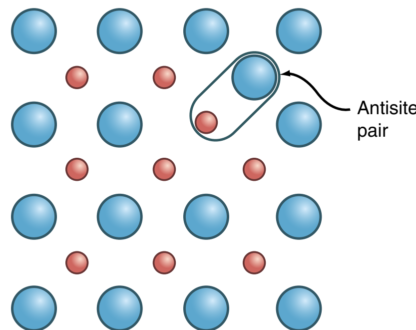

Fig. 4 Schematic representation of an anti-site pair in a binary crystal lattice.

process for the whole crystal. Thus, as the temperature changes, many thousands of vacancies are created/destroyed and new material containing many thousands of ions is formed. Thus, not simply that one new molecule is formed but there is also an increase in the volume of the crystal, which is why the lattice energy is part of the Schottky reaction.

The energy for the Schottky disorder reaction to proceed in an AB material is the energy to create one A site vacancy by removing an ion from the crystal to infinity plus the energy to create one B site vacancy by removing an ion from the crystal to infinity, plus the lattice energy associated with one unit of the AB compound. For example in Al_2O_3, the energy would be that associated with the sum of two Al vacancies plus three O vacancies plus the lattice energy of one Al_2O_3 formula unit. Again the vacancy species are assumed to be effectively infinitely separated.

In a crystalline material with more than one type of atom, each species usually occupies its own sublattice. If two different species are swapped, this produces an anti-site pair (see **Fig. 4**). For example, in an AB compound, one A atom is swapped with the B atom. While this would be of high energy for an AO compound, where A and O are of opposite charge (e.g., Mg^{2+} and O^{2-}), in an ABO_3 material where A and B may have similar or even identical positive charges, antisite energies can be small.

Author's personal copy

In general, the energies needed to form each type of disorder, in a given material, are different. Therefore, only one type of intrinsic disorder dominates: this is often described as the intrinsic disorder of the material. If one intrinsic process is of much lower energy than others it will dominate the equilibrium: this is useful when investigating other defect processes, as we will see later.

In most metals and metal alloys, Schottky disorder dominates due to the close packed nature of their crystal structure. In ceramics, both Schottky and Frenkel disorder are possible; for example, in NaCl and MgO (both with the rock salt structure) Schottky disorder dominates but in CaF_2 and UO_2 (both with the fluorite structure) anion Frenkel disorder dominates, while in $MgAl_2O_4$ spinel, anti-site disorder dominates. In Al_2O_3 the situation is too close to call and it is not clear if Frenkel or Schottky disorder dominates.[6]

1.02.2.5 Concentration of Intrinsic Defects

We start with the assumption that, for a given set of ions, their crystal structure represents the most stable arrangement of those ions in space. Thus, there is an enthalpy cost to form atomic defects: energy is expended in forming the defects. How then do defects form? The answer is related to free energy considerations; that is, the increase in the enthalpy of the system can be balanced with a corresponding increase in entropy and more particularly configurational entropy. Point defects in a crystal can therefore be described as entropically stabilized, and as such they are equilibrium defects (dislocations and grain boundaries, for example, are not equilibrium defects).

If the enthalpy of forming n Schottky pairs in an AB material is $n\Delta h$, the vibrational entropy is $nT\Delta s$, where T is temperature (in K), so that $n\Delta g_f = n\Delta h + nT\Delta s$, and the change in entropy associated with this reaction is ΔS_c, the change in Free Energy (ΔG) of the system (if we ignore pressure volume term effects) is;

$$\Delta G = n\Delta g_f - T\Delta S_c$$

If we assume that the entropy is all associated with configuration

$$\Delta S_c = k \ln \Omega$$

where k is Boltzmann's constant and Ω is the number of distinct ways that n Schottky pairs can be arranged in the crystal. If we assume that there are N "A" lattice sites (in defect chemistry terms, a lattice site means a position in the crystal that an ion will usually occupy in that crystal structure) the number of ways, Ω_A, of arranging n A-site vacancies is;

$$\Omega_A = \frac{N!}{n!(N-n)!}$$

As we have n B-site vacancies to distribute over N B-lattice sites, $\Omega_A = \Omega_B$. Thus, the total number of configurations is the product of Ω_A and Ω_A;

$$\Delta S_C = k \ln\left[\left(\frac{N!}{n!(N-n)!}\right)\left(\frac{N!}{n!(N-n)!}\right)\right] = 2k \ln\left(\frac{N!}{n!(N-n)!}\right)$$

where N and n are large, as they are when dealing with crystals, we can invoke Stirling's approximation, which states that $\ln(M!) = M \ln(M) - M$. Thus,

$$\Delta S_C = 2k[(N \ln (N) - N) - ((N-n) \ln (N-n) - (N-n)) - (n \ln (n) - n)]$$
$$\Delta S_C = 2k[N \ln (N) - (N-n) \ln (N-n) - n \ln (n)]$$

Therefore,

$$\Delta G = n\Delta g_f - 2kT[N \ln(N) - (N-n)\ln(N-n) - n \ln(n)] = n\Delta g_f - 2kT\left[N \ln\left(\frac{N}{N-n}\right) + n \ln\left(\frac{N-n}{n}\right)\right]$$

To find the equilibrium number of defects, we need to find the minimum of ΔG with respect to n (see Fig. 5). That is,

$$\left(\frac{\partial \Delta G}{\partial n}\right)_{T,P} = 0 = \Delta g_f - 2kT \ln\left(\frac{N-n}{n}\right)$$

Assuming that the number of defects is small in comparison to the number of available lattice sites then: $N - n \approx N$:

$$\frac{n}{N} = \exp\left(-\frac{\Delta g_f}{2kT}\right) = \exp\left(-\frac{\Delta h}{2kT}\right)\exp\left(\frac{\Delta s}{2k}\right)$$

If the concentration of defects is small, usually we assume that the energy associated with the change in vibrational entropy is negligible so that the concentration of defects (n/N) is dominated by the enthalpy of reaction;

$$[n] = \frac{n}{N} = \exp\left(-\frac{\Delta h}{2kT}\right)$$

However, this is not always a valid assumption and care must be taken. When defect concentrations are measured experimentally they are presented on an Arrhenius plot of ln(concentration) versus $1/T$, which yield straight lines with slopes that are proportional to the disorder enthalpy (see Fig. 6).

Author's personal copy

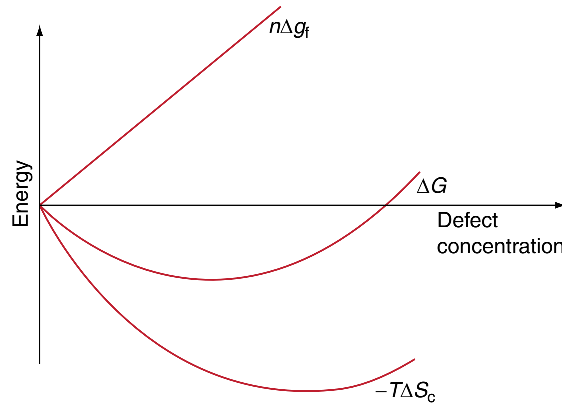

Fig. 5 Relationship of terms contributing to the defect free energy.

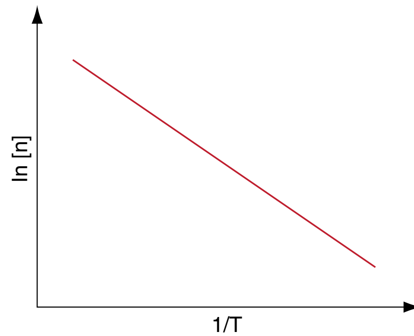

Fig. 6 Disorder enthalpy is proportional to the gradient of a ln[n] vs. 1/T graph.

1.02.3 Defect Reactions

1.02.3.1 Intrinsic Defects

Introducing a doping-agent to a crystal lattice can have a significant effect on the defect concentration within the material. As such doping represents a powerful tool in allowing us to engineer the properties of ceramic materials.

The concept of a solid solution, in which solute atoms are dispersed within a diluent matrix, is used in many branches of materials science. In many respects the defective lattice can be viewed as a solid solution in which the point defects are dissolved in the host lattice. The critical issue with such a view is in defining the chemical potential of an element. This is straightforward for the dopant species but is less clear when the species is a vacancy. This is circumvented by defining a virtual chemical potential, which allows us to write equations similar to those that describe chemical reactions. Within these defect equations it is critical that mass, charge and site ratio are all conserved.

Using Kröger-Vink notation we can describe the formation of Schottky defects in MgO in the following way;

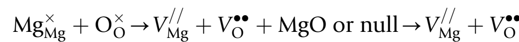

$$\mathrm{Mg}_{\mathrm{Mg}}^{\times} + \mathrm{O}_{\mathrm{O}}^{\times} \rightarrow V_{\mathrm{Mg}}^{//} + V_{\mathrm{O}}^{\bullet\bullet} + \mathrm{MgO} \text{ or null} \rightarrow V_{\mathrm{Mg}}^{//} + V_{\mathrm{O}}^{\bullet\bullet}$$

Note that in this case, the equation balances in terms of charge, chemistry and site.

Since this is a reaction, it may be described by a reaction constant "K", which is related to defect concentrations. In general the law of mass action[2] states that for a reaction.

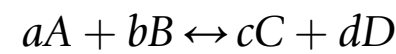

$$aA + bB \leftrightarrow cC + dD$$

$$\frac{[C]^c[D]^d}{[A]^a[B]^b} = K_{reaction} = \exp\left(-\frac{\Delta G}{kT}\right)$$

In the case of Schottky defects in MgO, we get

$$K_S = \left[V_{\mathrm{Mg}}^{''}\right]\left[V_{\mathrm{O}}^{\bullet\bullet}\right]$$

Additionally, charge neutrality dictates that

$$\left[V_{\mathrm{Mg}}^{''}\right] = \left[V_{\mathrm{O}}^{\bullet\bullet}\right]$$

Author's personal copy

And therefore

$$K_S = \left[V''_{Mg}\right]^2 = \left[V^{\bullet\bullet}_O\right]^2$$

So, if Δh is the enthalpy of the Schottky reaction, if we use our previous definition of concentration, $\frac{n}{N} = \exp\left(-\frac{\Delta h}{2kT}\right)$, then

$$\left[V^{//}_{Mg}\right] = \left[V^{\bullet\bullet}_O\right] = \exp\left(-\frac{\Delta h}{2kT}\right)$$

1.02.3.2 Effect of Doping on Defect Concentrations

Similar reactions can be written for extrinsic defects via the solution energy. For example, the solution of CoO in MgO, where the Co ion has a charge of 2+ and is therefore isovalent to the host lattice ion

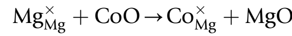

$$Mg^{\times}_{Mg} + CoO \rightarrow Co^{\times}_{Mg} + MgO$$

$$K_{solution} = \frac{\left[Co^{\times}_{Mg}\right][MgO]}{\left[Mg^{\times}_{Mg}\right][CoO]} \approx \exp\left(-\frac{\Delta h_{sol}}{kT}\right)$$

where Δh_{sol} is the solution enthalpy. The concentration of MgO in MgO = 1, and similarly that of CoO in CoO = 1. Henceforth these are omitted. For dilute solutions we can also approximate that $Mg^{\times}_{Mg} \approx 1$, so that

$$\left[Co^{\times}_{Mg}\right] \approx \exp\left(-\frac{\Delta h_{sol}}{kT}\right)$$

Consider the solution of Al_2O_3 in MgO. In this case, the Al ions have a higher charge and are termed aliovalent. These ions must be charge compensated by other defects, for example,

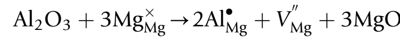

$$Al_2O_3 + 3Mg^{\times}_{Mg} \rightarrow 2Al^{\bullet}_{Mg} + V''_{Mg} + 3MgO$$

Then

$$\frac{\left[Al^{\bullet}_{Mg}\right]^2\left[V''_{Mg}\right]}{\left[Mg^{\times}_{Mg}\right]} = \exp\left(-\frac{\Delta h_{sol}}{kT}\right)$$

Since electroneutrality dictates that $[Al^{\bullet}_{Mg}] = 2[V''_{Mg}]$, it follows that,

$$\left[Al^{\bullet}_{Mg}\right] = \sqrt[3]{2}\,\exp\left(-\frac{\Delta h_{sol}}{3kT}\right)$$

1.02.3.3 Decrease of Intrinsic Defect Concentration Through Doping

When we considered the intrinsic defect reaction for MgO we wrote the defect reaction $K_S = [V''_{Mg}][V^{\bullet\bullet}_O]$. This implies that there is equilibrium between these two defect concentrations. Assuming that the enthalpy of the Schottky reaction, Δh = 7.7 eV,

$$\left[V^{//}_{Mg}\right]\left[V^{\bullet\bullet}_O\right] = \exp\left(-\frac{7.7}{kT}\right)$$

Now consider the effect that solution of 10 ppm Al_2O_3 has on MgO. The solution reaction implies that a concentration of 5 ppm of $V^{//}_{Mg}$ has been introduced into the lattice (i.e., $[V^{//}_{Mg}] = 5 \times 10^{-6}$). Therefore,

$$\left[V^{\bullet\bullet}_O\right] = 2 \times 10^5 \exp\left(-\frac{7.7}{kT}\right)$$

Thus, at 1000°C the $[V^{\bullet\bullet}_O] = 6.4 \times 10^{-26}$, compared to an oxygen vacancy concentration in pure MgO of 5.66×10^{-16}. The introduction of the extrinsic defects has therefore lowered the oxygen vacancy concentration by 10 orders of magnitude!

1.02.3.4 Defect Associations

So far we have assumed that when we form a set of defects through some interaction, while the defects will reside in the same lattice, somehow they do not interact to any significant extent. They are termed as non-interacting. This is valid in the dilute limit approximation, however, as defect concentrations increase, defects tend to form into pairs, triplets or possibly even larger clusters. Take for example the solution of Al_2O_3 into MgO.

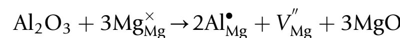

$$Al_2O_3 + 3Mg^{\times}_{Mg} \rightarrow 2Al^{\bullet}_{Mg} + V''_{Mg} + 3MgO$$

When the concentration is great enough,

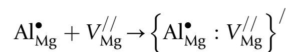

$$Al^{\bullet}_{Mg} + V^{//}_{Mg} \rightarrow \left\{Al^{\bullet}_{Mg} : V^{//}_{Mg}\right\}^{/}$$

Author's personal copy

A seen for solution energies, using the enthalpy associated with this pair cluster formation (the binding energy $\Delta h_{b\ pair}$), the reaction can be analyzed using mass action;

$$K_{binding\ pair} = \frac{\left[\left\{\mathrm{Al}^{\bullet}_{\mathrm{Mg}} : V''_{\mathrm{Mg}}\right\}'\right]}{\left[\mathrm{Al}^{\bullet}_{\mathrm{Mg}}\right]\left[V''_{\mathrm{Mg}}\right]} \approx \exp\left(-\frac{\Delta h_{b\ pair}}{kT}\right)$$

But since,

$$\left[\mathrm{Al}^{\bullet}_{\mathrm{Mg}}\right]^2\left[V^{//}_{\mathrm{Mg}}\right] = \exp\left(-\frac{\Delta h_{sol}}{kT}\right)$$

We have the relationship

$$\left[\left\{\mathrm{Al}^{\bullet}_{\mathrm{Mg}} : V^{//}_{\mathrm{Mg}}\right\}^{/}\right]\left[\mathrm{Al}^{\bullet}_{\mathrm{Mg}}\right] = \exp\left(-\frac{\Delta h_{binp} + \Delta h_{sol}}{kT}\right)$$

Which describes the solution process;

$$\mathrm{Al_2O_3} \rightarrow \mathrm{Al}^{\bullet}_{\mathrm{Mg}} + 3\mathrm{O}^{\times}_{\mathrm{O}} + \left\{\mathrm{Al}^{\bullet}_{\mathrm{Mg}} : V^{//}_{\mathrm{Mg}}\right\}^{/}$$

Further, it is possible to form a neutral triplet defect cluster, $\left\{\mathrm{Al}^{\bullet}_{\mathrm{Mg}} : V^{//}_{\mathrm{Mg}} : \mathrm{Al}^{\bullet}_{\mathrm{Mg}}\right\}^{\times}$, which has an binding enthalpy of $\Delta E_{b\ triplet}$ with respect to isolated defects so that

$$K_{binding\ triplet} = \frac{\left[\left\{\mathrm{Al}^{\bullet}_{\mathrm{Mg}} : V''_{\mathrm{Mg}} : \mathrm{Al}^{\bullet}_{\mathrm{Mg}}\right\}^{\times}\right]}{\left[\mathrm{Al}^{\bullet}_{\mathrm{Mg}}\right]^2\left[V''_{\mathrm{Mg}}\right]} \approx \exp\left(-\frac{\Delta h_{b\ triplet}}{kT}\right)$$

which leads to,

$$\left[\left\{\mathrm{Al}^{\bullet}_{\mathrm{Mg}} : V^{//}_{\mathrm{Mg}} : \mathrm{Al}^{\bullet}_{\mathrm{Mg}}\right\}^{\times}\right] = \exp\left(-\frac{\Delta h_{\mathrm{bint}} + \Delta h_{sol}}{kT}\right)$$

We now investigate the relative significance of defect clusters over isolated defects as a function of temperature for a fixed dopant concentration. For most systems there are a great number of possible isolated and cluster defects and the equilibria between them quickly becomes very complex. Solving such equilibria requires iterative procedures which are beyond the scope of this article.[7] Therefore, to illustrate the types of relationships that can occur, we will use the example of the binary $\left\{\mathrm{Ti}^{\bullet\bullet}_{\mathrm{Mg}} : V''_{\mathrm{Mg}}\right\}^{\times}$ cluster resulting from $\mathrm{TiO_2}$ solution in MgO via:

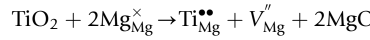

$$\mathrm{TiO_2} + 2\mathrm{Mg}^{\times}_{\mathrm{Mg}} \rightarrow \mathrm{Ti}^{\bullet\bullet}_{\mathrm{Mg}} + V''_{\mathrm{Mg}} + 2\mathrm{MgO}$$

and

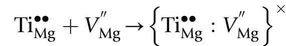

$$\mathrm{Ti}^{\bullet\bullet}_{\mathrm{Mg}} + V''_{\mathrm{Mg}} \rightarrow \left\{\mathrm{Ti}^{\bullet\bullet}_{\mathrm{Mg}} : V''_{\mathrm{Mg}}\right\}^{\times}$$

Then using:

$$\left[\mathrm{Ti}^{\bullet\bullet}_{\mathrm{Mg}}\right]\left[V''_{\mathrm{Mg}}\right]K_{binding\ pair} = \left[\left\{\mathrm{Ti}^{\bullet\bullet}_{\mathrm{Mg}} : V''_{\mathrm{Mg}}\right\}^{\times}\right]$$

and the electroneutrality condition

$$\left[\mathrm{Ti}^{\bullet\bullet}_{\mathrm{Mg}}\right] = \left[V''_{\mathrm{Mg}}\right]$$

yields

$$\left[\left\{\mathrm{Ti}^{\bullet\bullet}_{\mathrm{Mg}} : V''_{\mathrm{Mg}}\right\}^{\times}\right] = \left[\mathrm{Ti}^{\bullet\bullet}_{\mathrm{Mg}}\right]^2 K_{binding\ pair} \tag{1}$$

If the concentration of titanium ions on magnesium sites is x, so that $\mathrm{Mg}_{(1-2x)}\mathrm{Ti}_x\mathrm{O}$ is the formula of the material, then,

$$\left[\left\{\mathrm{Ti}^{\bullet\bullet}_{\mathrm{Mg}} : V''_{\mathrm{Mg}}\right\}^{\times}\right] = x - \left[\mathrm{Ti}^{\bullet\bullet}_{\mathrm{Mg}}\right] \tag{2}$$

Substituting (2) into (1) yields the quadratic equation,

$$K_{binding\ pair}\left[\mathrm{Ti}^{\bullet\bullet}_{\mathrm{Mg}}\right]^2 + \left[\mathrm{Ti}^{\bullet\bullet}_{\mathrm{Mg}}\right] - x = 0$$

Solving this in the usual manner allows us to determine $[\mathrm{Ti}^{\bullet\bullet}_{\mathrm{Mg}}]$ as a function of $K_{binding\ pair}$. If we now assume that $\Delta h_{b\ pair} = 1$ eV (a typical binding energy between charged pairs of defects in oxide ceramics), relationships between the concentration of the clusters and isolated substitutional ions can be determined as a function of either total dopant concentration, x, or temperature. These are shown in **Fig. 7**, which assumes a fixed temperature of 1000K and **Fig. 8** which assumes a fixed value of $x = 1 \times 10^{-6}$ and a range of temperature from 500K to 2000K.

Author's personal copy

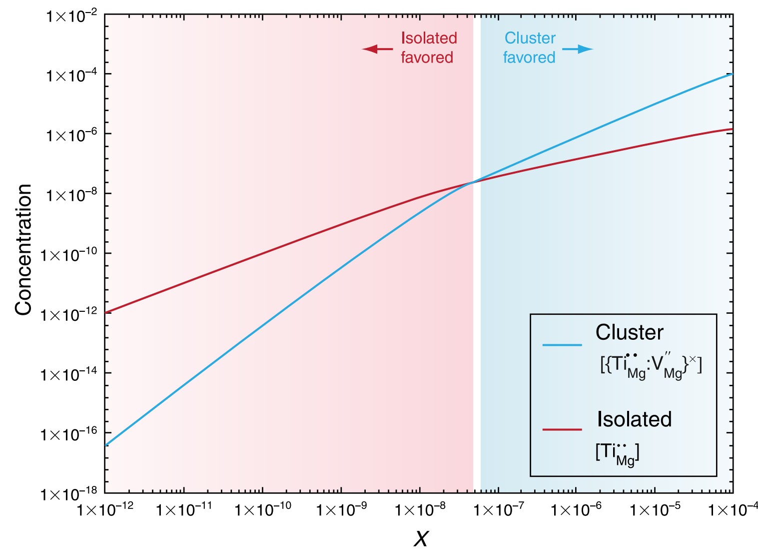

Fig. 7 Cluster and isolated defect concentration as a function of *x* at a temperature of 1000K.

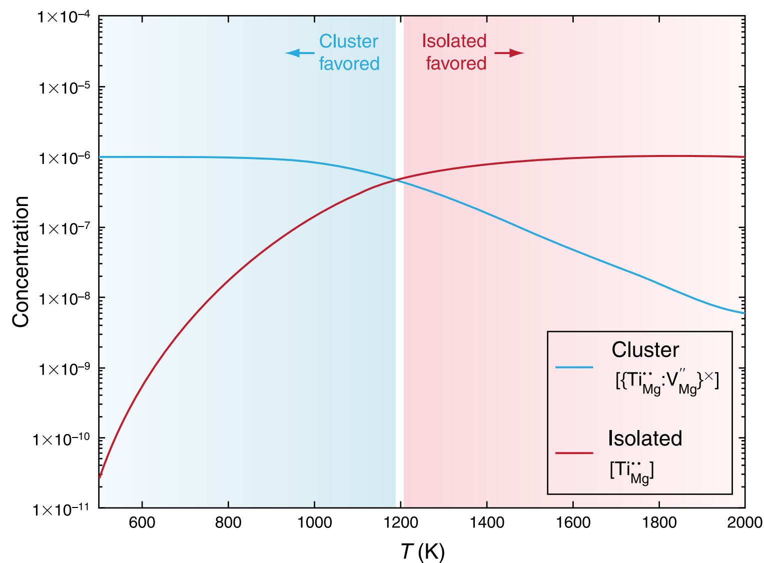

Fig. 8 Cluster and isolated defect concentration for $x = 1 \times 10^{-6}$ as a function of temperature.

1.02.3.5 Non-Stoichiometry

Although some materials such as MgO maintain the ratio between Mg and O very close to the stoichiometric ratio 1:1, other crystal structures such as UO_2 can tolerate large non-stoichiometries; $UO_{2\pm x}$ with $-0.35 < x < 0.25$ at the respective maximum hypo- and hyper-stoichiometry. The extent of the deviation from stoichiometry depends on how easily the host ions can assume charge states other than that associated with the host material, Fe^{3+} in the last case. Usually this comes down to how easily the cation can be oxidized or reduced. Associated with these reactions is the removal or introduction of oxygen from the atmosphere. For example, the reduction reaction follows;

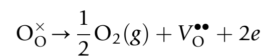

$$O_O^{\times} \rightarrow \frac{1}{2}O_2(g) + V_O^{\bullet\bullet} + 2e$$

where e represents a spare electron, which will reside somewhere in the lattice. For example, in UO_2, the electron is localized on a cation site forming a U^{3+} ion. This is usually written as U_U'. Similarly, the oxidation reaction is:

Author's personal copy

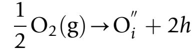

$$\frac{1}{2}O_2(g) \rightarrow O_i'' + 2h$$

where h represents a hole (i.e., where an electron has been removed since new oxygen species requires a charge of 2−). Again, in UO_2 the hole is often localized on the cation site, forming a U^{5+} ion, or $U_U^{\bullet}$. Thus, in UO_2, the oxidation reaction is:

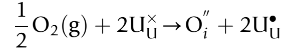

$$\frac{1}{2}O_2(g) + 2U_U^{\times} \rightarrow O_i'' + 2U_U^{\bullet}$$

If the enthalpy for the oxidation reaction is $\Delta h_{Ox,}$

$$\frac{[O_i''][U_U^{\bullet}]^2}{(P_{O_2})^{1/2}} = \exp\left(-\frac{\Delta h_{O_x}}{kT}\right)$$

where (P_{O_2}) is the partial pressure of oxygen (i.e., the concentration of oxygen in the atmosphere). Since electroneutrality gives us;

$$2\left[O_i''\right] = [U_U^{\bullet}]$$

$$\therefore \left[O_i''\right] \approx (P_{O_2})^{1/6}$$

Now if the majority of oxygen interstitials are associated with a single charge compensating U^{5+} species, that is, we have some defect clustering, the oxidation reaction will be;

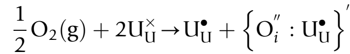

$$\frac{1}{2}O_2(g) + 2U_U^{\times} \rightarrow U_U^{\bullet} + \left\{O_i'' : U_U^{\bullet}\right\}'$$

and

$$\frac{[U_U^{\bullet}]\left[\left\{O_i'' : U_U^{\bullet}\right\}'\right]}{(P_{O_2})^{\frac{1}{2}}} = \exp\left(-\frac{\Delta h_{O_x}}{kT}\right)$$

which given that;

$$[U_U^{\bullet}] = \left[\left\{O_i'' : U_U^{\bullet}\right\}'\right]$$

implies that $[\{O_i'' : U_U^{\bullet}\}']$ is proportional to $(P_{O_2})^{1/4}$. Similar relations can be formulated for even larger clusters.

The defect concentration can be determined by measuring the self-diffusion coefficient. When this is related to the oxygen partial pressure via an $\ln(P_{O_2})$ versus $[\{O_i'' : U_U^{\bullet}\}']$ graph, the slope shows how the material behaves. For UO_2, the experimentally observed behavior is strongly stoichiometry dependent, with both 1/6 and 1/4 dependences observed in different regimes of temperature and stoichiometry.[8]

1.02.3.6 Peroxide Accommodated Hyper-Stoichiometry

So far in this section we have considered accommodation of oxygen non-stoichiometry via the formation of charge compensating hole or election species localized on a cation. This is possible in urania because of the variable charge state exhibited by uranium. For some oxides this mechanism is not available. For example, in thoria, while Th can exhibit a 3+ charge state, it's electronic configuration means Th^{4+} is not readily oxidized to Th^{5+}. In this case an alternative mechanism is preferred, that is, accommodation of excess oxygen via the formation of the peroxide species.[9] This occurs via the reaction.

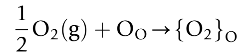

$$\frac{1}{2}O_2(g) + O_O \rightarrow \{O_2\}_O$$

Thus the excess oxygen is accommodated by forming a molecular species with an existing lattice oxygen ion. The peroxide ion carries the same overall charge as the O^{2-} lattice ion and is therefore a charge neutral species that does not require charge compensation.

The calculated solution enthalpy for this reaction in ThO_2 is 0.56 eV[9] so that total concentration of peroxide species will not be high and oxygen excess non-stoichiometry in thoria will not be great even at high P_{O2}. Conversely, in CeO_2 the predicted solution enthalpy is lower while in the monoxides CaO it is practically zero and in SrO a negative enthalpy is predicted leading to the formation of SrO_2.[10]

Charge-neutral peroxide formation was found to be the dominant mechanism for accommodation of excess oxygen in ternary perovskite materials.[11] Recent work on amorphous ZrO_2[12] indicates that peroxide formation may be particularly important for glasses and amorphous oxides, where a wider range on hyper-stoichiometry may be accommodated in the disordered lattice.

1.02.3.7 Lattice Response to a Defect

To formulate quantitative or often even qualitative models for defect processes in materials it is essential that lattice relaxation be taken into effect. Without lattice relaxation, the total energies calculated for defect reactions would be so great that we would have to conclude that no significant concentration of point defects would ever form in the material.[13]

Each defect has an associated defect volume. That is, each defect, when introduced into the lattice causes a distortion to its surrounding, which is manifested as a volume change arising due to the way in which the lattice responds, that is, how the lattice

Author's personal copy

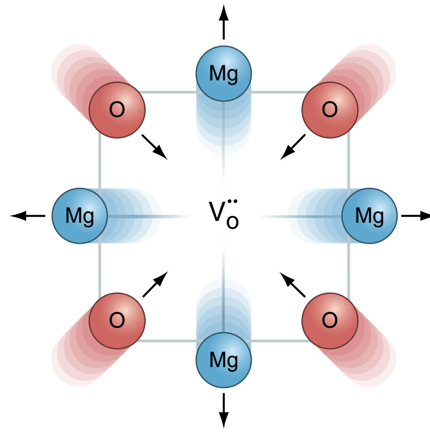

Fig. 9 Schematic of the lattice relaxations around an oxygen vacancy in MgO.

ions relax around the defect. In ionic materials, the response tends to be driven by electrostatic interactions. For example, vacancies in ionic materials usually result in positive defect volumes. Consider the example of a vacancy in MgO. The nearest neighbor cations are displaced outwards, away from the vacant site causing an increase in volume, whereas the second neighbor anions move inwards, albeit to a lesser extent (see Fig. 9).

What drives these ion relaxations is the changes in the Coulombic interactions due to defect formation. We say that the oxygen vacancy carries an effective positive charge because an O^{2-} has been removed and thus an electrostatic attraction between O^{2-} and Mg^{2+} is removed. Since ionic forces are balanced in a crystal, the outer O^{2-} ions now attract the Mg^{2+} away from the $V_O^{\bullet\bullet}$ defect site. In covalent materials, vacant sites result in atomic relaxations that are due to an incomplete complement of bonds forming; these are often termed "dangling bonds". In this case, the net result can be different from those in ionic solids and by way of an example, in silicon, a vacancy results in a volume decrease. Conversely, an arsenic substitutional atom causes an increase in volume.[14] In the case of uranium diboride, UB_2, the number of dangling bonds dictates, to a first approximation, the volume and energy of defect clusters of vacancies, and therefore also their concentration.[15] Finally, in a material such as ZrN or TiN, which exhibits both covalent and metallic bonding, the volume of a nitrogen vacancy is practically zero.[16]

Clearly the overall response of the lattice can be rather complicated. However, the defect volume can be determined fairly easily by applying the relationship[17,18];

$$u_P = -K_T V \left(\frac{df_V}{dV}\right)_T$$

where u_P is the defect volume (in Å^3), K_T is the isothermal compressibility (in eV/Å^3), V is the volume of the unit cell (in Å^3) and f_V is the Helmholz free energy of formation of the defect (in eV).

Finally, defect associations can also (but not necessarily) have a significant effect on defect volumes for a given solution reaction. For example, with Al_2O_3 solution in MgO, isolated $Al_{Mg}^{\bullet}$ and $V_{Mg}^{//}$ have the least effect on lattice parameter as a function of $[Al_{Mg}^{\bullet}]$ while formation of neutral $\{Al_{Mg}^{\bullet}:V_{Mg}^{//}\}^{\times}$ has the greatest effect (ten times greater reduction in lattice strain compared to the dilute defects at the same concentration).[19]

1.02.3.8 Defect Cluster Structures

So far we have ignored possible geometric preferences between the constituent defects of a defect cluster. Of course, for oppositely charged defects, electrostatic considerations would drive the defects to sit as close as possible to each other and would be described as a nearest neighbor configuration. However, as we saw in the previous section, defects can cause considerable lattice strain. Consequently the most stable defect configuration will be dictated by a balance between electrostatic and strain effects.

To illustrate cluster geometry preference and its effect on materials' properties, we will look at two cases in oxides which exhibit the fluorite lattice, UO_2 and cubic ZrO_2. First, consider bound Schottky clusters in which are three vacancy clusters $\{V_O^{\bullet\bullet} : V_U^{''''} : V_O^{\bullet\bullet}\}^X$, UO_2 with a formal charge of zero. These are also referred to as neutral tri-vacancy clusters. Schottky clusters are important in the microstructural evolution of nuclear fuel, as they dictate the intrinsic and extrinsic diffusion process in bulk UO_2, formation of pores and fission gas bubbles.[20]

Due to the opposite charge of $V_U^{''''}$ and the two $V_O^{\bullet\bullet}$, the vacancies tend to occupy neighboring site in the crystal lattice. There are three possible configurations in which $V_U^{''''}$ is surrounded by two $V_O^{\bullet\bullet}$ at the nearest neighbor position, as illustrated in Fig. 10. In UO_2, and in all other actinide oxides, the configuration where the vacancies are aligned in a line along the [111] direction, $SD_{[111]}$, is found to be the most energetically favorable.[21] This is largely because the anion vacancies have positive effective charge and repel each other. Of the nearest neighbor configurations around the cation vacancy, $SD_{[111]}$ is favored because it allows these anion vacancies to sit as far apart as possible. The positive charges of the anion vacancies are also "screened" by the presence of the cation

Author's personal copy

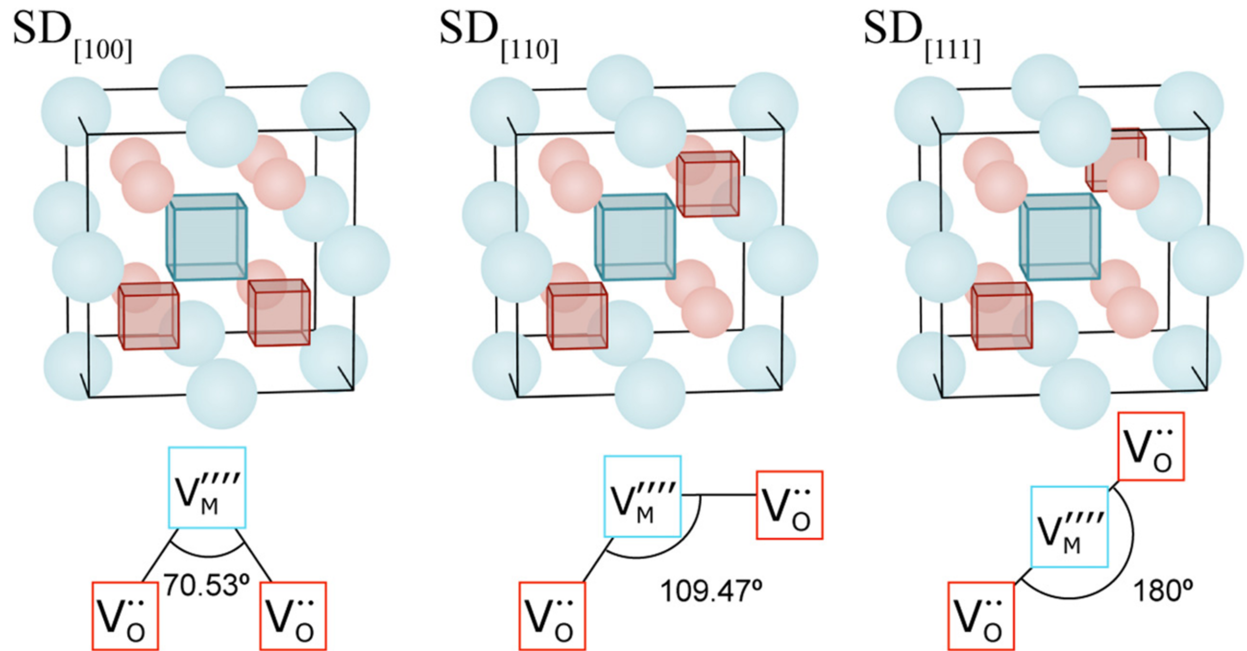

Fig. 10 Bound Schottky cluster configurations in the fluorite structure. Smaller red spheres represents oxygen, larger blue spheres represent U atoms. Boxes represents vacancies.

vacancy between them. This configuration, $SD_{[111]}$, is observed to be most stable for many other ionic compounds with fluorite structure, including non-oxide compounds.[21] Notably, there have been numerous reports of atomic scale simulations where the $SD_{[110]}$ defect appeared most stable, contrary to expectations. However, it was later found that those results were affected by spurious simulation artefacts, caused by insufficiency small simulation cells.

Bound Schottky clusters are also a low energy site to accommodate gaseous fission products, such as Xe and Kr, and the diffusivity of these species is bulk UO_2 is dictated by the migration of the Schottky cluster.[22] In this case, however, the most favorable configuration is found to be the $SD_{[100]}$, as it is the most compact and therefore provides the most space for the oversized noble gas atom.

Now we will consider simple defect pairs in the fluorite lattice, specifically in cubic ZrO_2. These will be formed between an oxygen vacancy, $V_O^{\bullet\bullet}$, and a trivalent ion, M^{3+}, that has substituted for a tetravalent lattice ion (i.e., $M_{Zr}^{/}$), thus partially charge compensating the oxygen vacancy. This doping process produces a technologically important fast ion conducting system, with oxygen ions transport via oxygen vacancy migration,[2,23] and is also observed at the interface between UO_2 pellets and Zr cladding of high burn-up fuel.

The lowest energy solution reaction that gives rise to the constituent isolated defects[24] is:

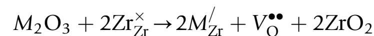

$$M_2O_3 + 2Zr_{Zr}^{\times} \rightarrow 2M_{Zr}^{/} + V_O^{\bullet\bullet} + 2ZrO_2$$

With the pair cluster formation following:

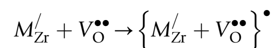

$$M_{Zr}^{/} + V_O^{\bullet\bullet} \rightarrow \left\{M_{Zr}^{/} + V_O^{\bullet\bullet}\right\}^{\bullet}$$

Fig. 11 shows the options for the pair cluster geometry, in which, if we fix the trivalent substitutional ion at the bottom left hand corner, the associated oxygen vacancy can occupy the 1st near neighbor, 2nd (or next) near neighbor or a 3rd near neighbor position.

Defect energy calculations have been used to predict the binding energy of the pair cluster as a function of the ionic radius[25] of the trivalent substitutional ion.[24] These suggest (see **Fig. 12**) that there is a change in preference from the near neighbor configuration to the second neighbor configuration as the ionic radius of the substitutional ion increases. The change occurs close to the Sc^{3+} ion. Furthermore, the binding energy of the near neighbor cluster falls as a function of radius, conversely the binding energy of the second neighbor cluster increases. Consequently the change in preference occurs at a minimum in binding energy. The third neighbor cluster is largely independent of ionic radius. Interestingly the minimum coincides with a maximum in the ionic conductivity, perhaps because the trapping of the oxygen vacancies as they move through the lattice is a minimum.[24]

The change in preference for the oxygen vacancy to reside in a first or second neighbor site is a consequence of the balance of two factors. First, the Coulombic attraction between the vacancy and the dopant substitutional ion, which always favors the first neighbor site, and is largely independent of ionic radius. Second, relaxation of the lattice, a crystallographic effect that always favors the second neighbor position. This is because, in the second neighbor configuration, the Zr^{4+} ion adjacent to the oxygen vacancy can relax away from the effectively positive vacancy without moving away from the effectively negative substitutional ion. Nevertheless, lattice

Author's personal copy

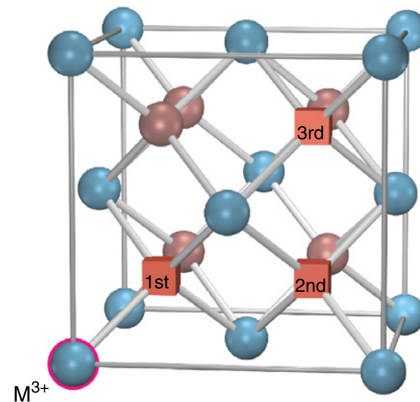

Fig. 11 First, second and third neighbor oxygen ion sites with respect to a substitutional ion (M^{3+}).

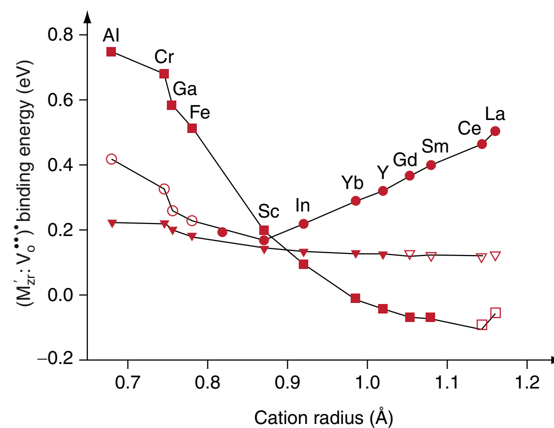

Fig. 12 Binding energies of M^{3+} dopant cations to an oxygen vacancy: ■ a 1st configuration; ● 2nd configuration and ▼ 3rd configuration. Open symbols represent calculations that required stabilization to retain desired configuration. Plot originally presented in reference Zacate, M.O., Minervini, L., Bradfield, D.J., Grimes, R.W., Sickafus, K.E., 2000. Solid State Ion. 128, 243.

relaxation in the first neighbor configuration still contributes an important energy term. However, in the first neighbor configuration, relaxation of oxygen ions is greatly hindered by the presence of larger trivalent cations, whilst small trivalent ions provide more space for relaxation. Thus, the relaxation preference for the second neighbor site increases in magnitude as ionic radius increases and consequently the second neighbor configuration becomes more stable compared to the first.[24]

This example shows that even in a simple system such as a fluorite, with a simple defect cluster, the factors that involved in determining cluster geometry become highly involved. Even so, we have so far only considered structural defects. Next we investigate the properties of electronic defects.

1.02.4 Electronic Defects

1.02.4.1 Formation

Electronic defects are formed when single atoms or small groups of atoms in a crystal have their electronic structure changed: electrons removed, added or excited from their ground state configuration into a higher energy state. Most often this involves a valence electron, although electrons from inner orbits can also be excited if sufficient energy is available. In either case, the state left by this transition, which is no longer occupied by an electron, is usually termed a hole. These defects can be generated thermally, optically, by radiation or through ion beam damage. The excited electron component may be localized on a single atomic site and if the electron is transferred to another center, it is represented as a change in the ionization state of the ion or atom to which it is localized. This is sometimes described as a small polaron or trapped electron. Such electronic defects might migrate through the lattice via an activated hopping process. An example of a small polaron electron is a Ce^{3+} ion in CeO_{2-x}.[26] Alternatively, the excited electron may be delocalized and move freely through the crystal. In this case the electron occupies a conduction band state, which is formed by the superposition of atomic wave functions from many atoms. This is the case with most semiconductor materials. Similarly, the hole may also be localized

Author's personal copy

to one atomic center and be represented as a change in the ionization state of the ion or atom. Holes may also move via an activated hopping process. An example is a Co^{3+} ion in $Co_{1-x}O$, or Mo^{5+} in MoO_3.[27] Similarly the hole may also be delocalized. Intermediate situations may occur with the hole or electron being localized to a small number of atoms or ions, (known as a large polaron), or a specific type of hole state associated with a particular chemical bond.

The relationship between doping and its influence on electronic defects is of great technological importance in the field of semiconducting materials. For example, doping silicon with defect concentrations in the order of parts per million is sufficient for most microelectronic applications. Incorporating a phosphorous atom in silicon results in a shallow state below the conduction band that will easily donate an electron to the conduction band. The remaining four valence electrons of the phosphorous dopant will form sp^3 hybrid bonds with the four neighboring tetrahedral silicon atoms. It has been suggested that the state from which the electron is removed is associated with the dopant species and its surrounding four silicon atoms, in other words it is associated with a cluster.[28]

1.02.4.2 Concentration of Intrinsic Electrons and Holes

Under equilibrium conditions, the number of electronic defects of energy E is given by,[2,3]

$$n(E) = N(E) \cdot F(E)$$

where $N(E)$ is the volume density of electronic levels that have energy E (known as the density of states) and $F(E)$ is the probability that a given level is occupied, called the Fermi-Dirac distribution function.

$N(E)$ is a function of energy. It is the maximum density of electrons of energy E allowed (per unit volume of crystal) by the Pauli exclusion principle. For a semiconductor, this has an approximate parabolic behavior close to the band edges (i.e., $N(E) \approx E^{1/2}$, refer to Fig. 13).

To determine N_c, the effective conduction band density of states, we need to integrate[2,3]

$$\int_E N_c(E)dE$$

$$N_c = 2\left(\frac{2\pi m_e^* kT}{h^2}\right)^{3/2} \approx 10^{19}\ \mathrm{cm}^{-3}$$

where m_e^* is the effective mass of an electron in the conduction band. Similarly, the effective valence band density of states is given by[2,3]

$$N_v = 2\left(\frac{2\pi m_h^* kT}{h^2}\right)^{3/2} \approx 10^{19}\ \mathrm{cm}^{-3}$$

where m_h^* is the effective mass of a hole in the valence band. Note, m_e^* and m_h^* are between 2 and 10 times greater than the mass of a free electron. Also, per volume, these densities are approximately four orders of magnitude less than the typical atom density in a solid.

The probability of occupying an energy state E is described by Fermi-Dirac statistics. The Fermi-Dirac distribution function is given by[2,3]

$$F(E) = \frac{1}{1 + \exp\left(\frac{E - E_f}{kT}\right)}$$

At T = 0K, F($E < E_f$) = 1 and F($E > E_f$) = 0. This is a step function, where all states below the Fermi level are occupied, and all

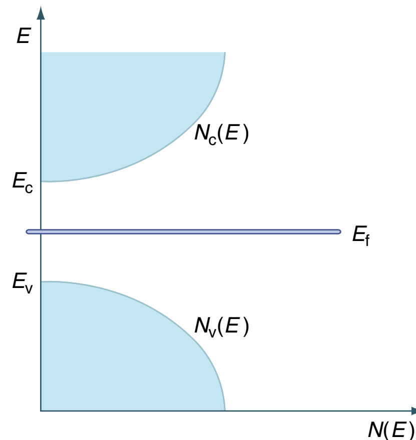

Fig. 13 Schematic representation of the density of states function N(E).

Author's personal copy

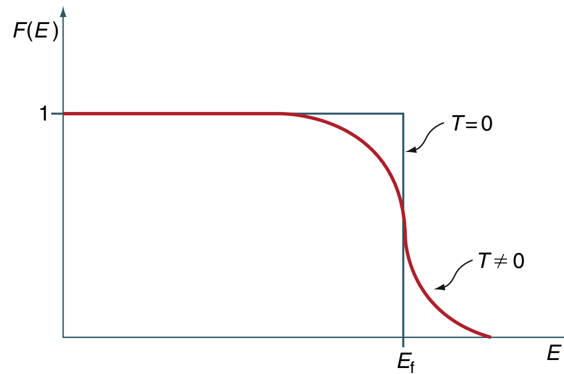

Fig. 14 Variation of the Fermi probability function with respect to the electron energy.

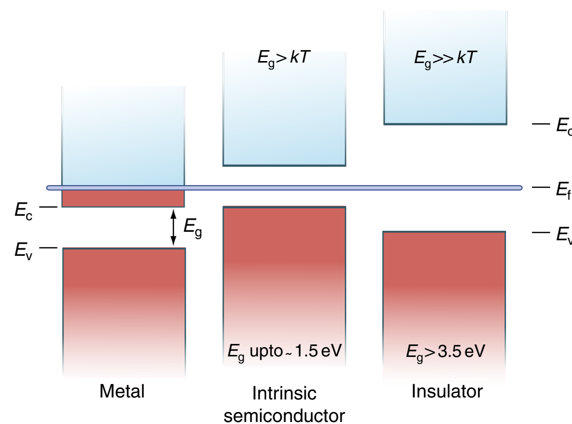

Fig. 15 Characteristic electron energy band levels for a metal, an intrinsic semiconductor and an insulator. Where E_c is the bottom of the conduction band, E_v is the top of the valence band, E_g is the band gap and E_f is the Fermi level.

states above it are empty, as represented in Fig. 14. At temperature above zero K, some energy levels above E_f are occupied, and some levels below E_f are empty. At the Fermi energy, the probability of the state being occupied, F(E), is ½.

1.02.4.3 Band Gaps

Materials can be classified by the occupancy of the energy bands (Fig. 15). In an insulator or a semiconductor an energy band gap, E_g, is between the filled valence band, E_v, and the unoccupied (at 0K) conduction band. In metals the conduction band is partially filled (refer to Fig. 15). Typical semiconductors have band gaps up to 1.5 eV, whereas when the band gap exceeds 3.5 eV the material is considered to be an insulator. Table 1 reports the band gaps of some important semiconductors (Ge, Si, GaAs, SiC, and UO_2) and insulators (MgO, $MgAl_2O_4$ and Al_2O_3).

1.02.4.4 Excited States

The definition for an electronic defect is effectively "a deviation from the ground state electronic configuration". The defects discussed in the Section 1.02.4.2 were holes and electrons. Here we consider defects where the excited species is localized around the atom from which it was excited.

If an electron is excited into a higher lying orbital, there must be a difference between the angular momentum of the ground state and excited state to accommodate the angular momentum of the photon that has been absorbed during the excitation process (conservation of angular momentum). For example, if the ground state is a singlet, the excited state may be a triplet. A simple example would be 2p → 3s excitation of an oxygen ion in MgO (Fig. 16).

Notice how the energy levels in Fig. 16 alter their energies between the ground state and excited states. Therefore, in this case it is not correct to estimate the energy difference between the ground state and excited states based on knowledge of only the ground state energy configuration.

Author's personal copy

Table 1 Band gaps of important semiconductors and insulators

Material	*Band gap (eV)*
Ge	0.66
Si	1.11
GaAs	1.43
UO_2	2.1
SiC	2.9
MgO	7.8
$MgAl_2O_4$	7.8
Al_2O_3	8.8

Note: Schoenes, J., 1978. J. Appl. Phys. 49, 1463. Chiang, Y.M., Birnie, D., Kingery, W.D., 1997. Physical Ceramics: Principles for Ceramic Science and Engineering. Cambridge: MIT Press.

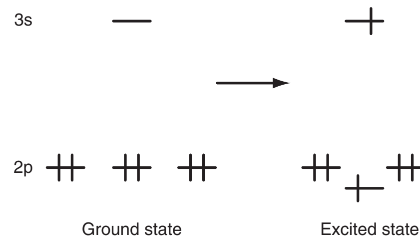

Fig. 16 The 2p → 3s excitation of an oxygen ion in MgO.

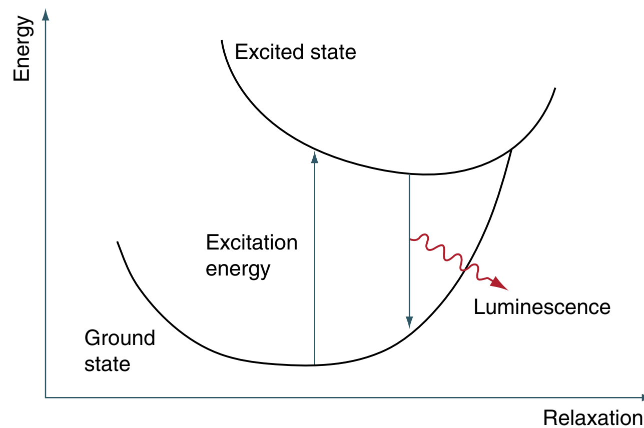

Fig. 17 The process of luminescence.

If the excitation energy is calculated based on the ground state ion positions this is known as the Franck-Condon vertical transition. When a photon is absorbed, the energy can be equal to this transition. However, the electron in the higher orbital will cause the forces between ions to be altered. Consequently, ions in the lattice will change their positions slightly, that is relaxation will occur. Such relaxation processes are known as non-radiative, that is light is not emitted. Notice that the total energy of the system in the excited state decreases. However, if the triplet excited state now decays back to the singlet ground state (a process known as luminescence,[29] see **Fig. 17**), locally the ions are no longer in their optimum positions for the ground state. The difference between the excitation energy and the luminescence energy is known as the Stokes Shift.[29]

Fig. 18 represents an example of an excited state electron in MgO, known as a self-trapped exciton.[30] The model uses the idea that an exciton is composed of a hole species and an excited electron. Notice that the excited electron has an orbit that is between the hole and its nearest neighboring cations. Thus, the hole is shielded from the cations. This means that the cations do not relax to the extent they would if there was a bare hole (the small relaxations are indicated by the arrows). Experimentally the excitation energy in MgO is 7.65 eV, the luminescence is 6.95 eV, which yields a small Stokes shift of only 0.7 eV.[31]

In comparison, a model for the exciton in alkali halides is shown in **Fig. 19**. In this case the exciton is composed of a V_k center (a hole shared between two halide ions) and an excited electron (the so-called $V_k + e$ model). However, notice how the two

Author's personal copy

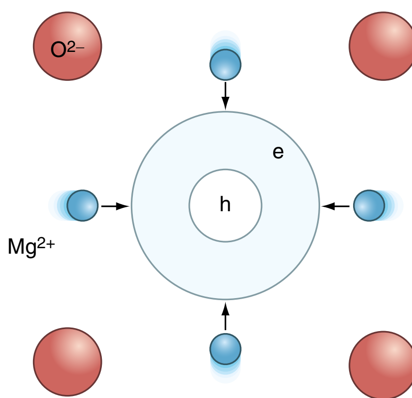

Fig. 18 A schematic representation of an exciton in MgO.

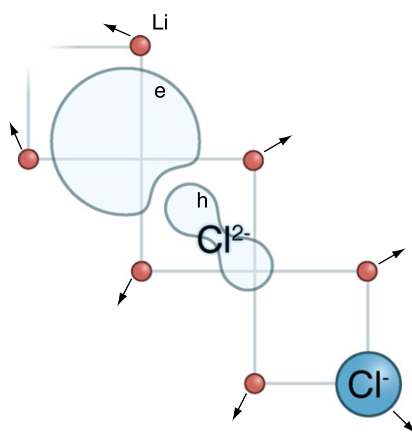

Fig. 19 A model for the exciton in alkali halides. The exciton is composed of a hole shared between two halide ions (V_k center) and an excited electron (the so-called V_k + e model). Interestingly, the two halide ions that comprise the V_k center are not displaced equally from their original lattice positions. Diagram derived from reference Shluger, A.L., Harker, A.H., Grimes, R.W., Catlow, C.R.A., 1992. Phil. Trans. R. Soc. Lond. A 341, 221.

halide ions that comprise the V_k center are not displaced equally from their original lattice positions. In fact one of the halide ions is essentially still on its lattice site while the other is almost in an interstitial site. Since calculations suggest that the hole is about 80% localized on this interstitial halide ion, it is almost an interstitial atom known as an H-center. Also, the electron is shifted away from the hole center and is sited almost completely in the empty halide site (called an F-center). As such the model is almost a Frenkel pair plus an electron localized at a halide vacancy (the so-called F-H pair model).

Whichever model is nearest to reality, V_k + e or F-H pair, it is clear that there is considerable lattice relaxation. This is reflected in the large Stokes shift. In LiCl, the optical excitation energy is 8.67 eV and the π-luminescence energy is only 4.18 eV leading to a Stokes shift of 4.49 eV.[32]

1.02.5 The Brouwer Diagram

1.02.5.1 Defects With Formal Charge States

So far we have considered both structural and electronic defects. In addition, we have derived the relationship between oxygen vacancies and the oxygen partial pressure, P_{O2}, which gives rise to non-stoichiometry. We now consider the equilibrium between isolated structural defects, electronic defects and P_{O2}. Of course, we have also considered the equilibrium that exists between isolated structural defects and defect clusters but defect clusters will not be considered in the present context. Nevertheless, defect clustering does play an important role in the equilibrium between electronic and structural defects and cannot, in a research context, be ignored.

In solving defect equilibria in the previous sections we have generally ignored the role that minority defects might have. For example, when considering Schottky disorder in MgO, which we know from experiments is the dominant defect formation process, the effect that oxygen interstitials might have was not taken into account.[2] This is certainly reasonable within the context of determining the oxygen vacancy concentration of MgO. The oxygen vacancy concentration is the important parameter to know when predictions of the oxygen diffusivity in MgO are required. However, minority defects may well play an important role in

Author's personal copy

other physical processes. For example, the electrical conductivity or resistivity will depend on the hole or electron concentration; these may be minority defects compared to oxygen vacancies but they are nevertheless crucial to know. Thus we must be concerned with four different defect processes[2] simultaneously:

(1) The dominant intrinsic structural disorder process (e.g., Schottky or Frenkel).
(2) The intrinsic electronic disorder reaction.
(3) The REDOX reaction.
(4) Dopant and impurity effects.

Again we begin by considering MgO. If we ignore impurity effects the three reactions are[2]:

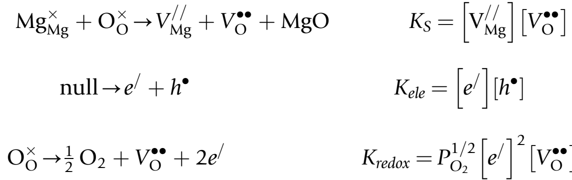

$$\mathrm{Mg}_{\mathrm{Mg}}^{\times} + \mathrm{O}_{\mathrm{O}}^{\times} \rightarrow V_{\mathrm{Mg}}^{//} + V_{\mathrm{O}}^{\bullet\bullet} + \mathrm{MgO} \qquad K_S = \left[\mathrm{V}_{\mathrm{Mg}}^{//}\right]\left[V_{\mathrm{O}}^{\bullet\bullet}\right]$$

$$\mathrm{null} \rightarrow e^{/} + h^{\bullet} \qquad K_{ele} = \left[e^{/}\right]\left[h^{\bullet}\right]$$

$$\mathrm{O}_{\mathrm{O}}^{\times} \rightarrow \tfrac{1}{2}\mathrm{O}_2 + V_{\mathrm{O}}^{\bullet\bullet} + 2e^{/} \qquad K_{redox} = P_{\mathrm{O}_2}^{1/2}\left[e^{/}\right]^2\left[V_{\mathrm{O}}^{\bullet\bullet}\right]$$

These equations contain six unknown quantities, four are defect concentrations, the other two variables are the P_{O2} and the temperature, which are experimental variables and are thus given. Of course, we must know the enthalpies of the defect reactions. Nevertheless, to solve these equations simultaneously we need a further relationship. This is provided by the electroneutrality condition, which, for MgO states that[2]:

$$2\left[V_{\mathrm{Mg}}^{//}\right] + \left[e^{/}\right] = 2\left[V_{\mathrm{O}}^{\bullet\bullet}\right] + \left[h^{\bullet}\right]$$

To make the problem more tractable, we now introduce the Brouwer approximations, which simplify the form of the electroneutrality condition. These effectively concern the availability of defects via the partial pressure of oxygen. For example, if the P_{O2} is very low, the REDOX reaction equilibrium will require that the $\left[V_{\mathrm{O}}^{\bullet\bullet}\right]$ and $\left[e^{/}\right]$ concentrations are relatively high so that these are the dominant positive and negative defect concentrations. Therefore for low P_{O2}[2];

$$\left[e^{/}\right] = 2\left[V_{\mathrm{O}}^{\bullet\bullet}\right]$$

Conversely at high P_{O2}, both oxygen vacancies and their charge compensating electrons must have relatively low concentrations and therefore the electroneutrality condition becomes dominated by the $[V_{\mathrm{Mg}}^{//}]$ and $[h^{\bullet}]$ defects so that[2];

$$\left[h^{\bullet}\right] = \left[V_{\mathrm{Mg}}^{//}\right]$$

Between these two regimes, the Brouwer approximation depends on whether structural or electronic defects dominate. In the case of MgO we know that Schottky disorder dominates over electronic disorder (as it is a good insulator) and therefore at intermediate values of P_{O2} the appropriate electroneutrality condition is;

$$\left[V_{\mathrm{O}}^{\bullet\bullet}\right] = \left[V_{\mathrm{Mg}}^{//}\right]$$

If the electronic disorder was dominant, this last reaction would be replaced by;

$$\left[e^{/}\right] = \left[h^{\bullet}\right]$$

We are now is a position to be able to construct a Brouwer diagram, sometimes also referred to as the Kröger-Vink diagram. This usually takes the form of *ln(defect concentration)* versus *ln*(P_{O2}) for various defect components at a constant temperature. In the case of MgO, from the above, the diagram will clearly have three regimes corresponding to the three Brouwer conditions (refer to **Fig. 20** and Ref. 2).

1.02.5.2 Oxidation States of Defects

The approximations used to define the three Brouwer regions, hold remarkably well for MgO and many other metal oxides. Sometimes, for some materials under certain T and P_{O2} conditions, there is no dominating defect. When this is the case, the Brouwer diagrams must be constructed without the above approximations. To that end, one must calculate the energy to form each individual defect, and each defect cluster if those are also considered. To account for the fact that some defects may adopt more than one oxidation state, their formation energies must be expressed as a function of the electron potential (the Fermi level) μ_e, which describes the energy cost or gain when removing (adding) a free electron in the material. In the most general form, the enthalpy of formation of a defect of charge q can be defined as:

$$\Delta h_f = \Delta E_{def} \pm \sum_{\alpha} n_{\alpha}\mu_{\alpha} + q\mu_e$$

where ΔE_{def} is the defect energy (the energy difference between a crystal containing the defect and a perfect crystal), n_{α} is the number of species α that were added or removed to form the defect, and μ_{α} is the chemical potential of that species. For a $V_{\mathrm{O}}^{\bullet\bullet}$ in

Author's personal copy

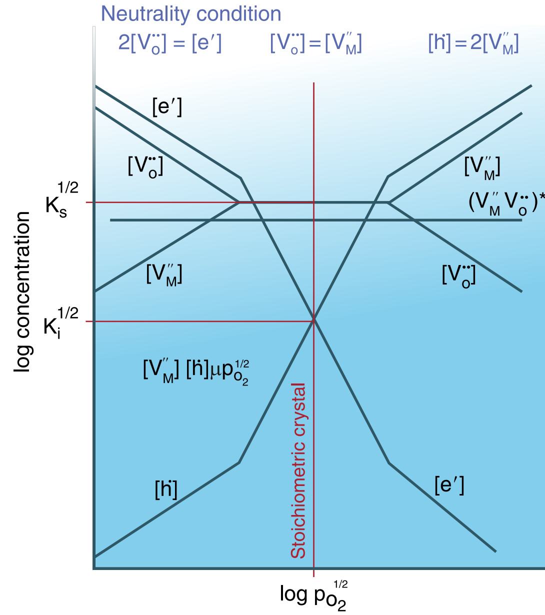

Fig. 20 The Brouwer diagram for MgO. Reproduced from Chiang, Y.M., Birnie, D., Kingery, W.D., 1997. Physical Ceramics: Principles for Ceramic Science and Engineering. Cambridge: MIT Press.

UO_2, the enthalpy of formation of the vacancy is expressed as

$$\Delta h_f = \Delta E_{def} - \mu_O + 2\mu_e$$

If the crystal is in thermodynamic equilibrium with the surrounding atmosphere, then we can state that

$$\mu_O = \frac{1}{2}\mu_{O_2}(T, p_{O_2})$$

which provides a direct link between defect concentration and temperature and oxygen partial pressure. The temperature dependence of μ_{O_2} can be expressed through the ideal gas law.

For defects that do not involve the removal or addition of O species, the relationship to μ_{O_2} is established through appropriate choice of reservoir of that species. For instance, the chemical potential of UO_2 can be expressed as a sum of the chemical potential of its constituent species.

$$\mu_{UO_2} = \mu_U + \mu_{O_2}(T, p_{O_2})$$

The Fermi level, μ_e, can take any value between the valence band maximum (VBM) and the conduction band minimum (CBM) of the material. Thus, the energy of charged defects varies linearly across the band gap of the material, while the energy of charge-neutral defects is independent on electron chemical potential. This is illustrated in **Fig. 21** for the case of Si impurities in MoO_3, where only the lowest energy charge states are shown at each Fermi level, considering both substitution and interstitial accommodation on three potential interstitial sites. This implies that in conditions where the Fermi level is near the conduction band (e.g., through n-type doping, or because of proximity to an interface with a material with higher workfunction), the Si interstitials will adopt neutral or even negative charge states, while the same defects are expected to exhibit positive charge states of 4+ under the opposite conditions. Repeating this exercise for oxygen vacancies in MgO presented earlier, would show that $V_O^{\bullet\bullet}$ exhibits lower formation energy than $V_O^{\bullet}$and $V_O^{\times}$ across the entire range of plausible fermi energies (i.e., the band gap of MgO).

The condition of global electroneutrality enables us to impose one further constraint: that the sum of the concentrations, c, of all charged defects must obey.

$$\sum_i q_i c_i = 0 \tag{3}$$

Since the formation energy of all charged defects, including electronic defects, depends on the Fermi level, for a given temperature and oxygen partial pressure, there is only one Fermi level, and therefore one set of defect concentrations, that satisfies electroneutrality. This can be calculated through an iterative self-consistent scheme, whereby a trial μ_e is used to predict the concentration of charged defects, then these are summed according to Eq. (3). If the total charge is positive/negative, a lower/higher μ_e is used in the following iteration.[33,34] This can be repeated until the total charges converges to electroneutrality within an acceptable accuracy (e.g., $\sum_i q_i c_i = 10^{-4}\,e$).

Iterating the procedure for a range of temperatures and/or oxygen partial pressures yields a complete Brouwer diagram, as shown for the case of Sb-doped tetragonal ZrO_2 in **Fig. 22**. In this case, the concentration of Sb in the material is kept at a constant 10^{-3} (atoms per formula unit). It is evident that the Sb is accommodated as a 3+ species at low P_{O2} (charge compensated by

Author's personal copy

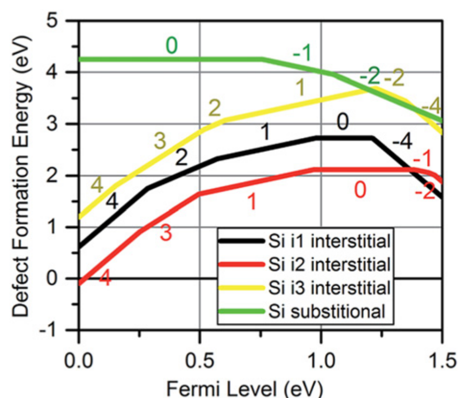

Fig. 21 Defect formation energy of Si defects in MoO_3. Labels represent charge state of defect, and for each defect position, only the lowest energy charge state is shown. Reproduced from Lambert, D.S., Murphy, S.T., Lennon, A., Burr, P.A., 2017. RSC Adv. 7, 53810.

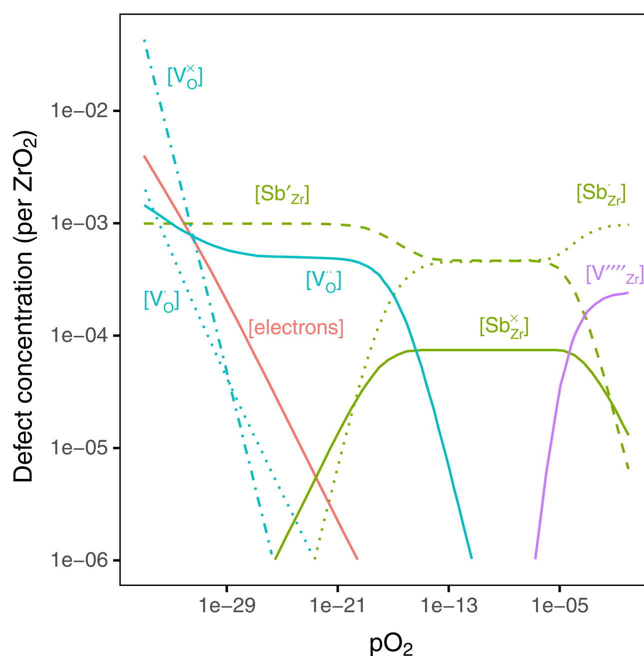

Fig. 22 The Brouwer diagram Sb-doped tetragonal ZrO_2. Reproduced from Bell, B.D.C., Murphy, S.T., Burr, P.A., *et al.*, 2016. Corr. Sci. 105, 36–43.

oxygen vacancies) and as a 5+ species at high P_{O2} (charge compensated by Zr vacancies), with an intermediate regime in which Sb'_{Zr} is charge compensated by $Sb^{\bullet}_{Zr}$. This self-balancing action of Sb dopants plays an important role in slowing down the water-side corrosion of Sb-containing Zr-alloy cladding.[35]

1.02.6 Transport Through Ceramic Materials

1.02.6.1 Diffusion Mechanisms

Diffusion in ceramic materials is a process made possible by defects and controlled by their concentrations and their mobility. Due to the existence of separate sublattices, cation and anion diffusion is restricted to take place separately (i.e., without exchange of anions and cations), which is one of the main differences with respect to diffusion in other materials.[36] Therefore, mechanistically diffusion theory is applied in ceramics by considering the anion and cation sublattices separately. Interestingly, it has recently been suggested[37] that where there is more than one cation sublattice, cations can move on an alternate sublattice through the formation of cation anti-site defects. Finally, it can be the case that ion transport in one of the sublattices is more pronounced. For example, in oxygen fast ion conductors (e.g., doped ZrO_2 or CeO_2 systems) oxygen self-diffusion is orders of magnitude faster than cation diffusion.[38–40]

Author's personal copy

Transport in crystalline materials requires the motion of atoms away from their equilibrium positions and therefore the role of point defects is significant.[36] For example, vacancies provide the space into which neighboring atoms in the lattice can jump,[41–43] although sometimes it is the interstitial defects that provide the transport mechanism.[36]

Diffusion mechanisms refer to the way an atom can migrate in a crystal through a connected series of hops from one position in the lattice to another, generally through an activated process that sees the ion move over an energy barrier. As such, it is mathematically represented as a Markov chain of jumps between states. The beginning and end points to each jump may be symmetrically identical and provide a contiguous pathway through the crystal but this need not be so. In some cases, the contiguous migration pathway may involve a number of non-identical steps. Nevertheless, in most materials the motion of an atom is restricted to a few paths.

There are three main mechanisms that are relevant to most ceramic systems: the interstitial, the interstitialcy and the vacancy-mediated mechanism. However, for completeness we will also briefly describe the collective and the interstitial-substitutional exchange mechanisms, which may be encountered in other classes of materials.[31]

In the interstitial mechanism, atoms initially at interstitial sites migrate by jumping from one interstitial site to a neighboring one (**Fig. 23**). At the completion of a single jump there is no permanent displacement of the other ions, although, of course, in the process of diffusion the extent of lattice relaxation is likely to have become greater to facilitate the saddle point configuration. In principle it is a simple mechanism as it does not require the existence of defects other than the interstitial ion, although it is possible that transient defects are produced if the lattice relaxation is great enough in the course of the jump. Interstitial diffusion is not common in ceramic materials but does occur if the interstitial species is small.

In the interstitialcy mechanism an interstitial atom displaces an atom from its normal substitutional site (**Fig. 24**). The displaced atom moves in turn to an interstitial site. This mechanism is important for the diffusion of dopants such as boron in silicon,[44] as well as for the self-diffusion of smaller ions in iono-covalent ceramics such as B in UB_2[15] and C in WC.[45] Similarly, in hyper-stoichiometric oxides, such as $La_2NiO_{4+\delta}$, it was predicted that oxygen diffuses predominantly via an interstitialcy mechanism.[40]

In the vacancy mechanism a host or substitutional impurity atom diffuses by jumping to a neighboring vacancy (**Fig. 25**). Vacancy-mediated diffusion is common in a number of systems – particularly ceramics with higher atomic density where interstitial defect energies are high. For example, the vacancy mechanism is important for the diffusion of substitutional impurities, for self-diffusion and the transport of *n*-type dopants in germanium[46,47] and for oxygen self-diffusion of a number of hypo-stoichiometric perovskite and fluorite related systems.[48] Of course, the vacancy mechanism requires the presence of lattice vacancies and therefore their concentration in the lattice will influence the kinetics.[43]

For intrinsic and dilute point defects, the chemical surroundings and energy landscape of the jumping atom do not change with subsequent jumps. This is also the case for extrinsic (dilute) interstitial defects. However, vacancy-mediated diffusion of extrinsic

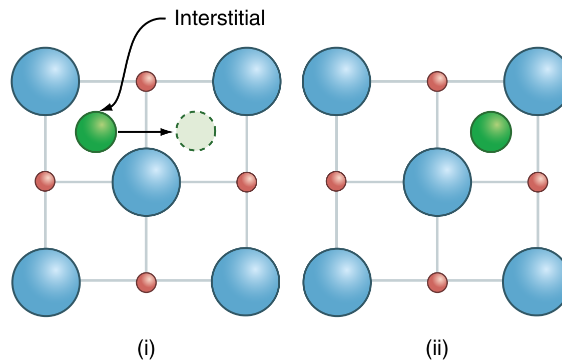

Fig. 23 The interstitial mechanism of diffusion. The red and blue atoms are lattice species.

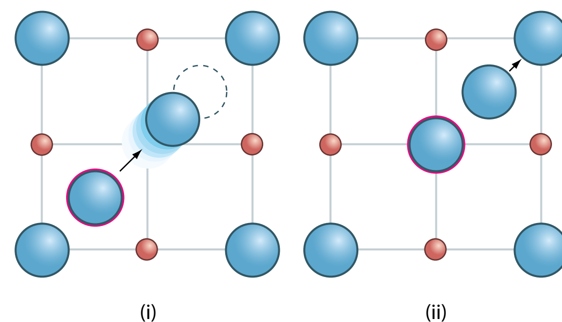

Fig. 24 The interstitialcy mechanism of diffusion. The red and blue ions are lattice species, the blue ion with the red perimeter is initially an interstitial species but becomes a lattice species.

Author's personal copy

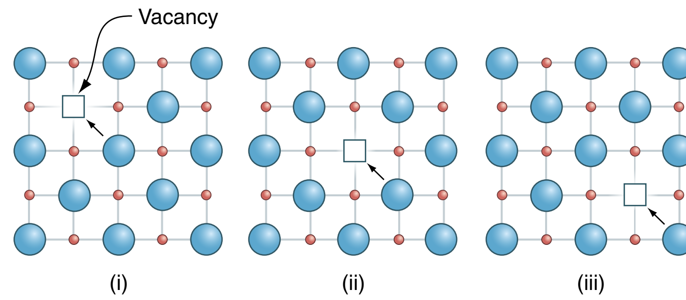

Fig. 25 The vacancy mechanism of diffusion. The red and blue ions are lattice species.

species (i.e., solutes) involves vacancy-solute interactions in many non-equivalent configurations. As the vacancy approached the solute, it experiences changes in its local surrounding, accompanied by an attraction to, or a repulsion from, the solute. This is also known as the binding energy between the solute and the vacancy. This leads to kinetic correlations, which significantly affect the overall solute transport. Mathematical frameworks have been developed recently to compute vacancy-mediated solute transport in crystals, including kinetic correlation.[49–51] This enables to calculate diffusivity and drag ratios (i.e., do vacancy and solute diffuse in the same direction or opposite directions?) from individual jump energies and solute-vacancy binding energies.

Collective mechanisms involve the simultaneous transport of a number of atoms. They can be found in ion conducting oxide glasses,[36] fluorapatite,[52] and have been predicted during the annealing of radiation damage.[53] Finally, in the interstitial-substitutional exchange mechanism the impurities can occupy both substitutional and interstitial sites.[36] One possibility for the interstitial atom is to migrate in the lattice until it encounters a vacant site, which it then occupies to become a substitutional impurity (dissociative mechanism).[36] Another possibility for the impurity interstitial atom is to migrate in the lattice until it displaces an atom from its normal crystallographic site thus forming a substitutional impurity and a host interstitial atom (kick-out mechanism). The interstitial-substitutional mechanism has been encountered for zinc diffusion in silicon and gallium antimonide.[60]

Naturally, there are potential energy barriers hindering the motion of atoms in the lattice. The activation energy associated with the barriers may be overcome by providing thermal energy to the system. The jump frequency ω of a defect is given by[3,54]

$$\omega = \nu \exp\left(-\frac{\Delta H_m}{k_B T}\right)$$

where ΔH_m is the migration enthalpy required to transport the defect from an initial equilibrium position to a saddle point and ν is the vibrational frequency. In real materials the atomic transport may be locally affected by interactions with other defects especially if the defect concentration is high.[55–57]

1.02.6.2 Diffusion Coefficient

The temperature dependence of the diffusion coefficient has an Arrhenius form:

$$D = D_0 \exp\left(-\frac{H_a}{k_B T}\right)$$

where H_a is the activation enthalpy of diffusion and D_0 is the diffusion pre-factor that contains all entropy terms and is related to the attempt frequency for migration. The activation enthalpy is the sum of the formation enthalpy (H_f) of the migrating species and its migration enthalpy (H_m).

$$H_a = H_f + H_m$$

H_m, is the energy barrier between an initial state and a final state of the diffusion process. For a system with a complex potential energy landscape, a number of different paths may need to be considered when calculating H_m. The formation energy, H_f, represents the energetic cost to construct a defect in the lattice (which may well require a complete Frenkel or Schottky process to occur), as defined in Section 1.02.5.

For solid solutions with a given composition, if the diffusion involves only an extrinsic interstitial species migrating from one interstitial site to an adjacent interstitial site, the activation enthalpy of diffusion is composed only of the migration enthalpy, since the concentration of species is fixed and it is temperature-independent. In comparison, for vacancy-mediated diffusion, the solutes are trapped in substitutional positions and form a cluster with one or more vacancies. In such a situation diffusion requires the formation of a vacancy in addition to the migration of the vacancy and the cluster. In cases where solutes may occupy both interstitial and substitutional positions, then the total diffusivity would be the sum of the two processes, weighed by the respective partition functions, such that the sum of interstitials and substitution concentrations must add up to the total concentration of the solute.[58]

In some cases, the formation energy contribution to the activation energy may be discounted, if the concentration of the diffusing defects is controlled by an extrinsic process (i.e., not thermally activated), such as aliovalent doping or radiation damage. For instance, the introduction of trivalent Gd^{3+} in UO_2 leads to an increase in oxygen vacancies, $V_O^{\bullet\bullet}$ as dominant charge-compensation mechanism for Gd_U' substitution. Specifically, a concentration of charge-compensating oxygen vacancies

Author's personal copy

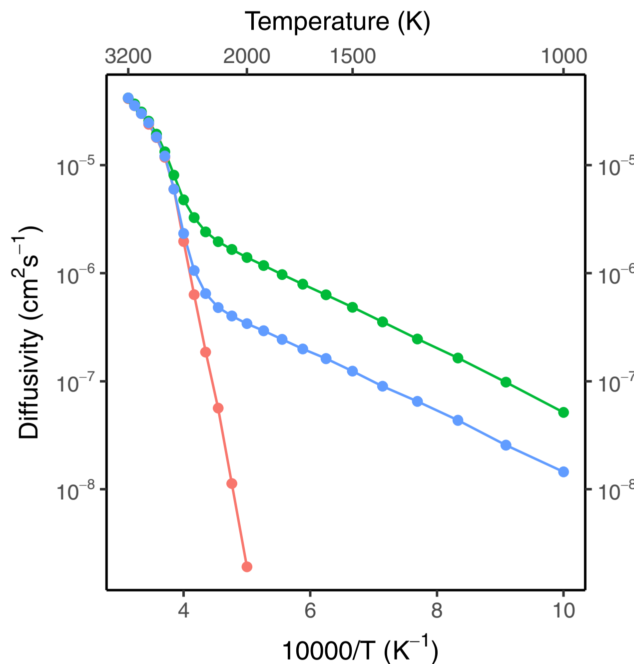

Fig. 26 Oxygen self-diffusion in UO_2 with 0%, 1% and 2% Gd additions, calculated from molecular dynamics simulations. Reproduced from Galvin, C.O.T., Cooper, M.J.D., Rushton, M.W.D., Grimes, R.W., 2018. J. Nucl. Mater. 498, 300–306.

equal to $\left[V_O^{\bullet\bullet}\right] = \frac{1}{2}\left[Gd_U'\right]$ are introduced into the material, which are in addition to the contributions from intrinsic processes such as Frenkel pairs and Schottky defects. At low temperatures, the extrinsic processes dominate over the intrinsic (thermally activated) processes. As a result, for most temperatures the vacancy-mediated oxygen self-diffusivity in Gd-doped UO_2 is orders of magnitude greater than in undoped UO_2 (see **Fig. 26**).[59] At temperatures above the super-ionic transition, the difference between doped and undoped UO_2 becomes small, as oxygen Frenkel pairs become the dominant defect process.

1.02.7 Summary

Point defects are ubiquitous: as intrinsic species they are a consequence of equilibrium, but usually they are far more numerous, incorporated as extrinsic species formed as a consequence of fabrication conditions. Slow kinetics mean that impurities are trapped in ceramic materials, typically once temperatures drop below 800K, although this value is quite material dependent. The intentional incorporation of dopants into a crystal lattice can be used to fundamentally alter a whole range of processes: this includes the transport of ions, electrons and holes. As a result, diffusion rates and electrical conductivity can be persuaded to increase or decrease by many orders of magnitude.[1,2] Other mechanical or radiation tolerance related properties can also be changed radically.

This article has provided the framework for understanding the properties of point defects. From the concentration of equilibrium intrinsic species, dopant ions and their interdependence, defect association to form clusters and non-stoichiometry. In each case these defects alter the lattice surrounding them, with atoms being shifted from their perfect lattice positions in response to the specific defect type. Electronic defects have been described; electrons and holes formed by doping but also states formed by excitation. Structural defects and electronic defects are considered together through Brouwer diagrams. Finally, we considered the transport of ions through the lattice, via different processes, all of which require the formation of point defects.

1.02.8 Recommended Reading

In addition to references, readers are referred to the following texts the detail the behavior of defects in inorganic materials.

W. Van Gool, Principles of Defect Chemistry of Crystalline Solids, Academic Press, New York (1966).

A.M. Stoneham, Theory of Defects in Solids: Electronic Structure of Defects in Insulators and Semiconductors, Oxford University Press, Oxford (2001).

R.J.D. Tilley, Defect Crystal Chemistry and its Applications, Blackie & Son, Glasgow (1987).

F. Agullo-Lopez, C.R.A. Catlow and P.D. Townsend, Point Defects in Materials, Academic Press, San Diego (1988).

N.N. Greenwood, Ionic Crystals Lattice Defects and Nonstoichiometry, Butterworth, London (1970).

H. Schmalzried, Solid State Reactions, Academic Press, New York (1974).

P. Kofstad, Nonstoichiometry, Diffusion and Electrical Conductivity in Binary Metal Oxides, Wiley, New York (1972).

Author's personal copy

See also: 1.01 Fundamental Properties of Defects in Metals. 1.16 Ab Initio Electronic Structure Calculations for Nuclear Materials. 6.10 Radiation Effects on the Physical Properties of Dielectric Insulators for Fusion Reactors

References

1. Kingery, W.D., Bowen, H.K., Uhlmann, D.R., 1976. Introduction to Ceramics. New York: Wiley.
2. Chiang, Y.M., Birnie, D., Kingery, W.D., 1997. Physical Ceramics: Principles for Ceramic Science and Engineering. Cambridge: MIT Press.
3. Kittel, C., 1996. Introduction to Solid State Physics. New York: Wiley.
4. Hull, D., Bacon, D.J., 2001. Introduction to Dislocations, fourth ed. Butterworth-Heinemann.
5. Kröger, F.A., Vink, H.J., 1956. In: Seitz, F., Turnbull, D. (Eds.), Solid State Physics, vol. 3. New York: Academic Press.
6. Harding, J.H., Atkinson, K.J.W., Grimes, R.W., 2003. J. Am. Ceram. Soc. 86, 554.
7. Ball, J.A., Pirzada, M., Grimes, R.W., *et al.*, 2005. J. Phys.: Condens. Matter 17, 7621.
8. Cooper, M.W.D., Murphy, S.T., Andersson, D.A., 2018. J. Nucl. Mater. 504, 251–260.
9. Middleburgh, S.C., Lumpkin, G.R., Grimes, R.W., 2013. Solid State Ion. 253, 119–122.
10. Middleburgh, S.C., Lagerlof, K.P.D., Grimes, R.W., 2013. J. Am. Ceram. Soc. 96, 308–311.
11. Middleburgh, S.C., Karatchevtseva, I., Kennedy, B.J., *et al.*, 2014. J. Mater. Chem. A 2, 15883–15888.
12. Rushton, M.J.D., Ipatova, I., Evitts, L.J., Lee, W.E., Middleburgh, S.C., 2019. RSC Adv. 9, 16320–16327.
13. Royal Society of Chemistry, 1989. J. Chem. Soc., Faraday Trans. 2: Mol. Chem. Phys. 85, 335–579. (see papers in the special issue) doi:10.1039/F298985FP043.
14. Chroneos, A., Grimes, R.W., Tsamis, C., 2006. Mater. Sci. Semicond. Process. 9, 536.
15. Burr, P.A., Kardoulaki, E., Holmes, R., Middleburgh, S.C., 2019. J. Nucl. Mater. 513, 45–55.
16. Ashley, N.J., Grimes, R.W., McClellan, K.J., 2007. J. Mater. Sci. 42, 1884.
17. Minervini, L., Zacate, M.O., Grimes, R.W., 1999. Solid State Ion. 116, 339–349.
18. Catlow, C.R.A., Corish, J., Jacobs, P.W.M., Lidiard, A.B., 1981. J. Phys. C 14, L121.
19. Vyas, S., Grimes, R.W., Binks, D.J., Rey, F., 1997. J. Phys. Chem. Solids 58, 1619.
20. Bès, R., Martin, P., Vathonne, E., *et al.*, 2015. Appl. Phys. Lett. 106, 114102.
21. Burr, P.A., Cooper, M.W.D., 2017. Phys. Rev. B 96, 094107.
22. Perriot, R., Metthews, C., Cooper, M.W.D., *et al.*, 2019. J. Nucl. Mater. 520, 96–109.
23. Goodenough, J.B., 2000. Nature 404, 821.
24. Zacate, M.O., Minervini, L., Bradfield, D.J., Grimes, R.W., Sickafus, K.E., 2000. Solid State Ion. 128, 243.
25. Shannon, R.D., 1976. Acta. Cryst. A32, 751.
26. Tuller, H.L., Nowick, A.S., 1977. J. Phys. Chem. Solids 38, 859.
27. Tahini, H.A., Tan, X., Lou, S.N., *et al.*, 2016. ACS Appl. Mater. Interfaces 8, 10911.
28. Schwingenschlogl, U., Chroneos, A., Schuster, C., Grimes, R.W., 2010. Appl. Phys. Lett. 96, 242107.
29. Stoneham, A.M., 1975. Theory of Defects in Solids. Oxford: Clarendon.
30. Shluger, A.L., Grimes, R.W., Catlow, C.R.A., Itoh, N., 1991. J. Phys.: Condens. Matter 3, 8027.
31. Rachko, Z.A., Valbis, T.A., 1979. Phys. Status Solidi B 93, 161.
32. Shluger, A.L., Harker, A.H., Grimes, R.W., Catlow, C.R.A., 1992. Phil. Trans. R. Soc. Lond. A 341, 221.
33. Murphy, S.T., Hine, N.D.M., 2014. Chem. Mater. 26, 1629–1638.
34. Youssef, M., Yildiz, B., 2012. Phys. Rev. B 86, 144109.
35. Bell, B.D.C., Murphy, S.T., Burr, P.A., *et al.*, 2016. Corr. Sci. 105, 36–43.
36. Mehrer, H., 2007. Diffusion in Solids. Berlin Heidelberg: Springer.
37. Murphy, S.T., Uberuaga, B.P., Ball, J.A., *et al.*, 2009. Solid State Ion. 180, 1.
38. Rupasov, D., Chroneos, A., Parfitt, D., *et al.*, 2009. Phys. Rev. B 79, 172102.
39. Miyoshi, S., Martin, M., 2009. Phys. Chem. Chem. Phys. 11, 3063.
40. Chroneos, A., Parfitt, D., Kilner, J.A., Grimes, R.W., 2010. J. Mater. Chem. 20, 266.
41. Bracht, H., Nicols, S.P., Walukiewicz, W., *et al.*, 2000. Nature 408, 69.
42. Weiler, D., Mehrer, H., 1984. Philos. Mag. A 49, 309.
43. Chroneos, A., Bracht, H., 2008. J. Appl. Phys. 104, 093714.
44. Sadigh, B., Lenosky, T.J., Theiss, S.K., *et al.*, 1999. Phys. Rev. Lett. 83, 4341.
45. Burr, P.A., Oliver, S.X., 2019. J. Eur. Ceram. Soc. 39, 165–172.
46. Brotzmann, S., Bracht, H., 2008. J. Appl. Phys. 103, 033508.
47. Chroneos, A., Bracht, H., Grimes, R.W., Uberuaga, B.P., 2008. Appl. Phys. Lett. 92, 172103.
48. Kilner, J.A., Irvine, J.T.S., 2009. Chapter 35 New oxide cathodes and anodes. In: Vielstich, W., Gasteiger, H.A., Yokokawa, H. (Eds.), Handbook of Fuel Cells – Advances in Electrocatalysis, Materials, Diagnostics and Durability, vol. 5-6. John Wiley & Sons.
49. Nastar, M., 2005. Philos. Mag. 85, 3767–3794.
50. Trinkle, D., 2017. Philos. Mag. 97, 2514–2563.
51. Schuler, T., Messina, L., Nastar, M., 2020. Comput. Mater. Sci. 172, 109191.
52. Jackson, M.L., Jay, E.E., Rushton, M.J.D., Grimes, R.W., 2014. J. Mater. Chem. A 2, 16157.
53. Uberuaga, B.P., Smith, R., Henkelman, G., *et al.*, 2005. Phys. Rev. B 71, 104102.
54. Vineyard, G.H., 1957. J. Phys. Chem. Solids 3, 121–127.
55. Brotzmann, S., Bracht, H., Lundsgaard Hansen, J., *et al.*, 2008. Phys. Rev. B 77, 235207.
56. Chroneos, A., Grimes, R.W., Uberuaga, B.P., Bracht, H., 2008. Phys. Rev. B 77, 235208.
57. Bernardi, F., dos Santos, J.H.R., Behar, M., 2007. Phys. Rev. B 76, 033201.
58. Jain, A.C.P., Burr, P.A., Trinkle, D.R., 2019. Phys. Rev. Mater. 3, 033402.
59. Galvin, C.O.T., Cooper, M.J.D., Rushton, M.W.D., Grimes, R.W., 2018. J. Nucl. Mater. 498, 300–306.
60. Conibeer, G.J., Willoughby, A.F.W., Hardingham, C.M., *et al.*, 1996. Zinc diffusion in tellurium doped gallium antimonide. JEM. 25, 1108–1112.